INVESTIGATION OF MULTIPORT BIDIRECTIONAL DC-DC CONVERTERS IN HYBRID VEHICLES

A DISSERTATION

Submitted in partial fulfillment of the requirements for the award of the degree of

INTEGRATED DUAL DEGREE

In

ELECTRICAL ENGINEERING

(With Specialization in Power Electronics)

By

SARVAGYA AGRAWAL

(11212013)

DEPARTMENT OF ELECTRICAL ENGINEERING

INDIAN INSTITUTE OF TECHNOLOGY ROORKEE

ROORKEE – 247 667 (INDIA)

MAY, 2016

CANDIDATE'S DECLARATION

I hereby declare that the work carried out in this dissertation entitled "**INVESTIGATION OF MULTIPORT BIDIRECTIONAL DC-DC CONVERTERS IN HYBRID VEHICLES**" submitted in partial fulfilment of the requirements for the award of the degree of Integrated Dual Degree (IDD) in Electrical Engineering with specialization in Power Electronics, submitted to the Department of Electrical Engineering, Indian Institute of Technology Roorkee, is an authentic record of my own work carried out under the guidance and supervision of Dr. S. P. Singh, Professor, Department of Electrical Engineering, Indian Institute of Technology Roorkee and all the works embodied in this thesis has not been submitted elsewhere for the award of any other degree.

Date: 24th May, 2016

Place: Roorkee **SARVAGYA AGRAWAL**

CERTIFICATE

This is to certify that the above statement made by the candidate is correct to the best of my knowledge and belief.

(**Dr. S. P. Singh**)

Professor,

Department of Electrical Engineering,

Indian Institute of Technology Roorkee

Roorkee-247667, India

ACKNOWLEDGEMENT

This thesis is a part of my M.Tech. Dissertation "Investigation of Multiport Bidirectional DC-DC Converters in Hybrid Vehicles" for the partial fulfilment of the requirements for the award of the Integrated Dual Degree in Electrical Engineering. I wish to affirm my deep sense of gratitude to my guide Dr. S. P. Singh, Professor, Department of Electrical Engineering, IIT Roorkee, for his intuitive, meticulous and benevolent guidance at all stage of my dissertation work. I wholeheartedly thank him for his kindly co-operation in scrupulously scrutinizing the manuscript and his valuable suggestions throughout my dissertation work. His knowledge has proved to be very useful for me to do the dissertation work appropriately.

Nevertheless, I dedicate my sincere thanks to my friend Abhilash Kulkarni for his incredible help and continuous support to carry out my dissertation work. I humbly acknowledge the help of all those who were involved directly or indirectly with my dissertation work.

SARVAGYA AGRAWAL

Enrolment No. 11212013

IDD Electrical (EPE)

ABSTRACT

The demand for versatile electrical energy management systems that interface diverse energy sources, energy storage elements and loads, is increasing because of their potential applications in hybrid electric vehicle (HEVs) and fuel cell vehicles (FCVs), renewable energy generation systems and uninterruptible power supplies. The voltage levels and the voltage-current characteristics of the energy sources and the storage elements are normally different from those of the loads. Therefore, a power electronics system to interface sources, storage elements and loads need to be incorporated into energy management systems.

In this report a novel Multi-port converter interfacing a photovoltaic array, battery and a DC load is proposed. It is composed of a uni-directional DC port for interfacing photovoltaic array, and two bi-directional DC port for interfacing battery and DC load. Compared to the traditional stand-alone photovoltaic power system, this system exhibits the advantages of better protection and more efficient control on charge/discharge of the battery. Furthermore, it can make better use of solar energy and realize energy management of the system. The key point of energy management for the system is to control the bi-directional converter efficiently, where bi-directional voltage and current must be controlled. In this report, the bi-directional control strategy of bi-directional converter is proposed, which operates at three operation modes: Buck (charge battery), Boost (discharge battery), and shut-down (SD). Maximum power point tracking control is used to extract the maximum power from the Photovoltaic array. Single power processing stage with multiple power ports offers an opportunity to make the whole system simpler, compact and more efficient. Finally, a simulation of 250W and 5 HP converter is built to verify the theoretical analysis and the control strategies. The simulation is tested for variable load and variable irradiance.

CONTENTS

LIST OF FIGURES

LIST OF ACRONYMS

DC	Direct Current
HEV	Hybrid Electric Vehicle
EV	Electric Vehicle
PV	Photovoltaic
MPPT	Maximum Power Point Tracking
STC	Standard Test Condition
OC	Open Circuit
P and O	Perturb and Observe
INC	Incremental Conductance
MOSFET	Metal Oxide Semiconductor Field Effect Transistor
PI	Proportional Integral
SOC	State of Charge
PWM	Pulse Width Modulation

LIST OF SYMBOLS

Ir	Irradiance
P_{pv}	Power supplied by PV panel
I_{mp}	PV panel current at maximum power
V_{mp}	PV panel voltage at maximum power
V_{oc}	Open circuit voltage
D	Duty ratio
T	Time
f	Frequency of the converter

CHAPTER 1: INTRODUCTION

1.1 Research Motivation

1.1.1 Renewable Energy Applications

Due to the rapid consumption of traditional fossil fuels, the energy crisis and environmental pollution become more severe. Renewable energy sources such as photovoltaic arrays, wind turbines and fuel cells are rich in nature, resulting in the advantages of zero emissions gaining more and more attention. Solar and wind power, they are the world's fastest growing energy resources. Today's photovoltaic arrays and wind turbines are the most advanced modern technology with modular design and quick installation. Since these are intermittent renewable energy sources, when combined with another renewable energy source can increase the certainty of continuous supply, because the individual characteristics of these sources are complementary to each other.

In recent years, much effort has been made to discover a Renewable clean energy sources around the world, and solar power is considered to be such an ideal and lasting source. Since 1970, solar photovoltaic power generation has received a great deal of attention and experienced impressive progress. Solar photovoltaic power generation will ease the energy crisis, reduce environmental pollution, and will play an important role in improving the greenhouse effect.

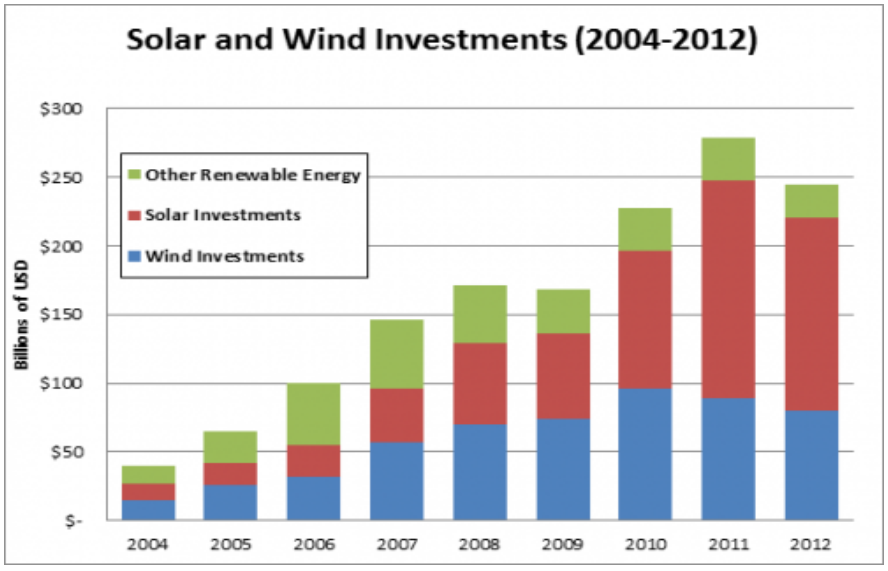

Figure 1.1 Investment in various renewable sources.

The ever-increasing demand for low-cost energy and growing anxiety about environmental problems, photovoltaic based systems are being progressively employed in various applications both at domestic and commercial levels. As shown in Figure 1.1, most of investment is made to deploy solar panels as compared to any other sources of renewable energy.

1.1.2 Advantages of Hybrid Electric Vehicles

The idea of replacing many of the cars on the road with clean commuter vehicles has affected most manufacturers of cars to start the development of cheap electric cars with as low price as possible. Electric vehicles use stored energy of battery or other types of energy storage systems for vehicle thrust and provide a clean and safe alternative to the internal combustion engine. Now the government has already imposed restrictions in many places on the use of highly contaminated vehicles, and vehicles with only a very low-emission are allowed to operate. In addition, many governments have begun to offer financial subsidies and tax cuts to promote the use of electric vehicles (EV). Society about a cleaner, renewable transportation is a priority for many countries. This is certainly a major problem for the automobile manufacturers around the world in response to the government.

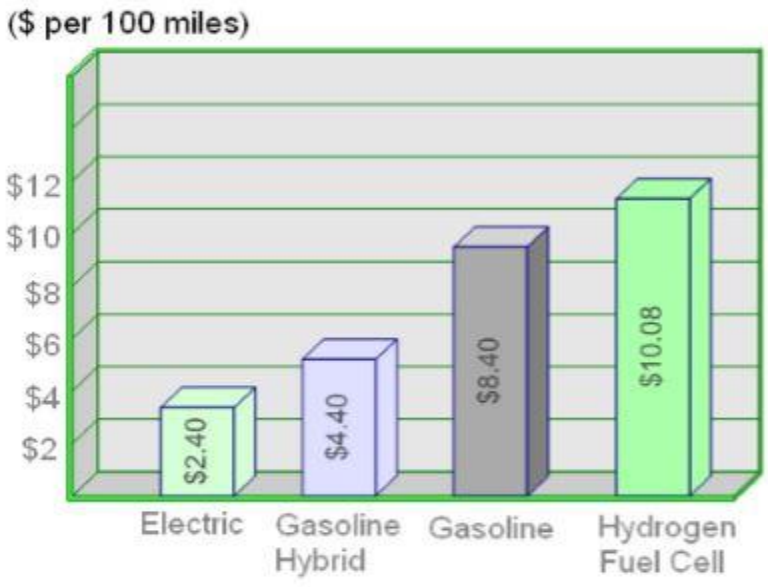

Figure 1.2 Equivalent costs per distance of different vehicles.

Figure 1.2 shows the money costs for different types of cars, per 100 miles route. I.e. for a 100 miles route with a gasoline car, it is necessary an equivalent money of 8.40 dollar,

while double distance can be covered for the equivalent sum of money in hybrid electric car. Moreover, a pure electric car, can cover three to four times distance as compared to gasoline car (with the same amount of money). However, even if the manufacture and the energy costs of an electric car could be cheaper than a normal car, they will certainly not be cheaper until their sales will be as higher as a diesel or gasoline car.

EVs provides high energy efficiency. In general, the overall energy conversion efficiencies from crude oil to vehicle motion are about 9-18%. While EVs, can perform efficiently by converting the kinetic energy of motor to electric energy of the source with an efficiency of nearly 25% through regenerative. (Including the efficiency of the electrical energy generation process). The overall process is presented in the next Figure 1.3.

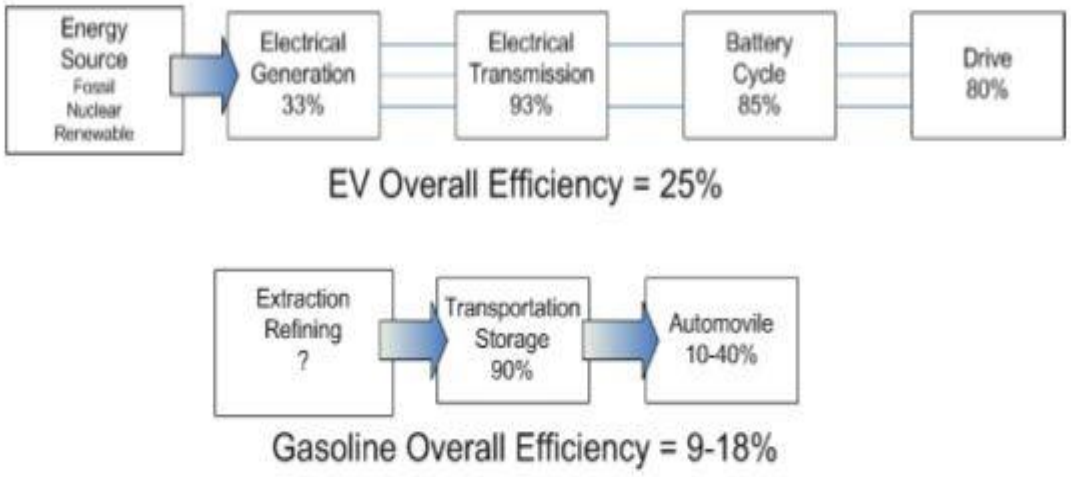

Figure 1.3 Energy conversion efficiency.

1.2 Literature Review

This section provides the review of the research that has already been conducted in the past years. This section comprises of two subsections for photovoltaic system and Multi-port converters review respectively. The review of photovoltaic systems escalates from their development to their P-V and I-V characteristics and finally the control schemes that are used. The review of multi-port converter comprises of its various topologies, types and control systems.

1.2.1 Review Based on Development of Photovoltaic Systems

Sera et al (2007) demonstrated the construction of photovoltaic panel using the five parameter single diode model, based on the model parameters he predicted the characteristics of photovoltaic panel under different irradiance and temperature conditions.

Villalva, M.G. Gazoli et al (2009) presented a method for simulation and modelling of photovoltaic systems. He also discussed the ways of calculating the panel series and parallel resistance.

Weidong Xiao et al (2004) discussed a modelling process to demonstrate the performance characteristics of the photovoltaic panel.

Trishan Esram et al (2007) discussed the various MPPT techniques to harness the maximum power from the photovoltaic panel. He described all the techniques that are being used to track the maximum power point.

1.2.2 Review Based on Topologies of Multi-port Converters

J. L. Duarte et al (2006) presented the various topologies of multi-port bidirectional converters and also discussed their advantages over conventional two-port converters.

Luca Solero et al (2004) proposed a multi-port converter for a hybrid drive train and discussed various methods of modelling and simulation of the same.

Zhiling Liao et al (2008) discussed the control strategies of a bidirectional DC-DC converter for interfacing photovoltaic panel in stand-alone applications.

F. Caricchi et al (1994) presented an experimental study on maintain a constant DC bus voltage by means of a bidirectional DC-DC converter. He also discussed the regenerative braking in a DC motor drive using bidirectional DC-DC converter.

1.3 Objective of the Thesis

This thesis provides a detailed study of the design, implementation and control of a three-port bidirectional DC-DC converter, interfacing a renewable source (photovoltaic), a battery and a load. This thesis broadly covers the following:

- Mathematical modelling of a photovoltaic system and the study of its characteristics under changing irradiation and temperature.

- Algorithms to harness the maximum power for any environmental condition by tracking the maximum power point.
- Design and analysis of a multi-port converter having unidirectional source and bidirectional ports for load and battery.
- Develop and implement the control strategy of the bi-directional port to manage the power flow between the source, load and the battery.
- Develop a MATLAB simulation model to verify the control strategy and test it of various loads under changing environmental conditions.
- Hardware implementation of the Simulink model and comparison of the hardware and simulation results to verify the simulation.

1.4 Thesis Organization

This thesis comprises of seven chapters. Each chapter provides a detailed study about mathematical modelling, design and control strategies of photovoltaic panels and multi-port converters.

Chapter 1 describes the need of hybrid vehicles which provided the motivation for the thesis, objective of the thesis has been discussed and thesis organization is presented.

Chapter 2 explains the detailed mathematical model of a photovoltaic cell, changes in P-V and I-V characteristics of PV module due to environmental conditions and describes the various maximum point tracking algorithms used to harness the maximum power.

Chapter 3 presents the advantages of multi-port converter over conventional two-port converters and their application. Discuss various topologies used depending upon the voltage and current demands. Finally, the control strategy of multi-port converter is discussed.

Chapter 4 describes the proposed three-port converter topology used and the control strategies that are being deployed to manage the power flow between all the ports.

Chapter 5 MATLAB simulation circuit and results of multi-port converter for variable irradiance, variable load and separately excited DC motor as load.

Chapter 6 presents the hardware implementation of the multi-port converter, detailed circuitry of the various components used and their tuned parameters.

Chapter 7 presents the conclusion of the thesis and provide some future scope of the topic.

CHAPTER 2: PHOTOVOLTAIC SYSTEMS

2.1 Photovoltaic Panels

Photovoltaic panels are composed of many photovoltaic cells. Photo voltaic cells convert solar light photons into electricity. Photovoltaic solar cells realise two functions: photo generation of charge carriers (electrons and holes) in a light-absorbing material, and separation of the charge carriers to a conductive contact that will transmit the electricity [10]. Photovoltaic cells are electrically connected in series and/or parallel circuits to generate higher voltages, currents and power levels. PV cell is the fundamental building block of PV systems. PV cell circuits are sealed in an environmentally protective laminate to make Photovoltaic modules. Photovoltaic panels include one or more PV modules assembled as a pre-wired, field-installable unit. PV array is the complete power generation device, consisting any number of photovoltaic modules and panels.

The performance of PV modules and arrays are generally rated according to their maximum DC power output (watts) under Standard Test Conditions (STC). Standard Test Conditions are defined as operating temperature of 25^0 C (77^0 F), and incident solar irradiance level of 1000 W/m^2 and under Air Mass 1.5 spectral distribution The actual performance of PV modules is 85 to 90 percent of the STC rating as the environmental conditions are not always standard in the fields they are operating .

2.2 Modelling of Photovoltaics Panel

The PV cell behaves similarly to a non-linear DC current source, it supplies variable power which depends, on the deviation of the temperature and irradiation [9]. The equivalent circuit of PV cells can be represented by either the venin's circuit or by Norton's circuit. The equivalent circuit of PV cell is as shown in Figure 2.1.

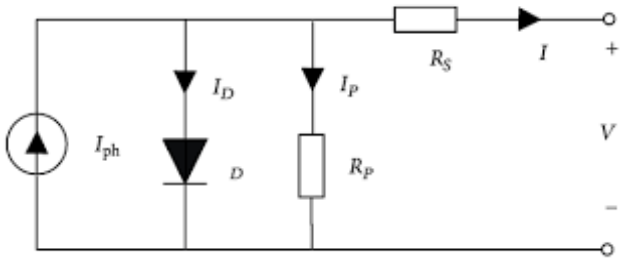

Figure 2.1 Equivalent circuit diagram of photovoltaic cell.

The model does not take into account the internal losses of the current. A diode is connected in anti-parallel with the light generated current source. The output current I is obtained by Kirchhoff law:

$$I = I_{ph} - I_D \tag{2.1}$$

I_{ph} is the photocurrent ,

I_D is the diode current

$$I_D = I_0\left[\exp\left(\frac{V}{A.N_s.V_T}\right)-1\right] \tag{2.2}$$

V is the voltage imposed on the diode.

$$V_T = k.T_c/q \tag{2.3}$$

I_0 is the reverse saturation or leakage current of the diode (A),

V_T = 26 mV at 300 K for silisium cell,

T_c is the actual cell temperature (K),

k is Boltzmann constant 1.381×10^{-23} J/K,

q is electron charge (1.602×10^{-19} C),

N_s is the number of PV cells connected in series.

In reality, it is impossible to neglect the series resistance Rs and the parallel resistance RP because of their impact on the efficiency of the PV cell and the PV module. When RS is taken into consideration, equation (2) should take the next form:

$$I_D = I_0\left[\exp\left(\frac{V + I.R_s}{A.N_s.V_T}\right)-1\right] \tag{2.4}$$

By applying Kirchhoff law, current will be obtained by the equation:

$$I = I_{ph} - I_D - I_p \tag{2.5}$$

The output current of a module containing N_s cells in series will be:

$$I_D = I_0\left[\exp\left(\frac{V + I.R_s}{A.N_s.V_T}\right)-1\right] - \frac{V + R_s.I}{R_p} \tag{2.6}$$

2.3 Effect of temperature and irradiance on solar cell characteristics

The *P–V* curve and *I–V* curve of PV panel corresponding to different temperatures and at constant insolation are shown in Figure 2.2 and 2.3. The output power of the PV panel decreases with the increase in temperature as depicted, this implies that a cooler panel produces more power than a comparatively hot panel. With increase in cell temperature the open circuit voltage decreases, while short circuit current slightly increases with cell temperature.

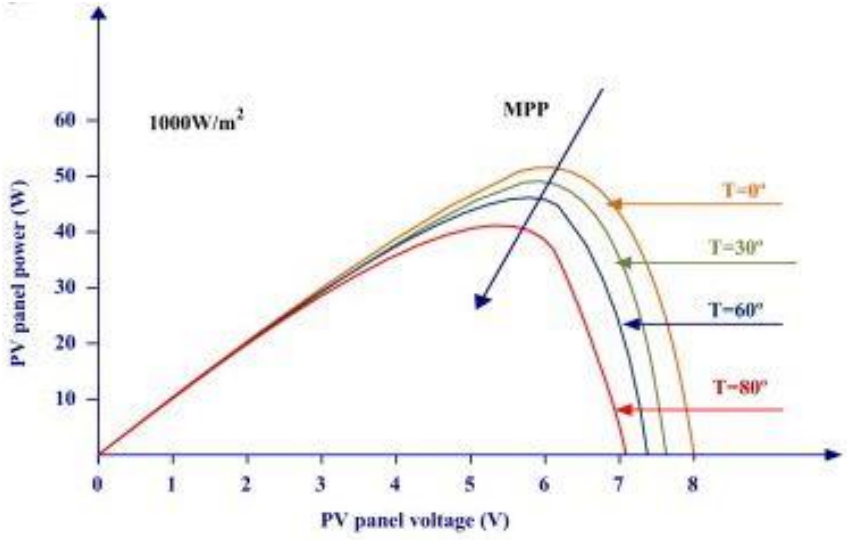

Figure 2.2 P–V characteristic at constant insolation and different temperatures.

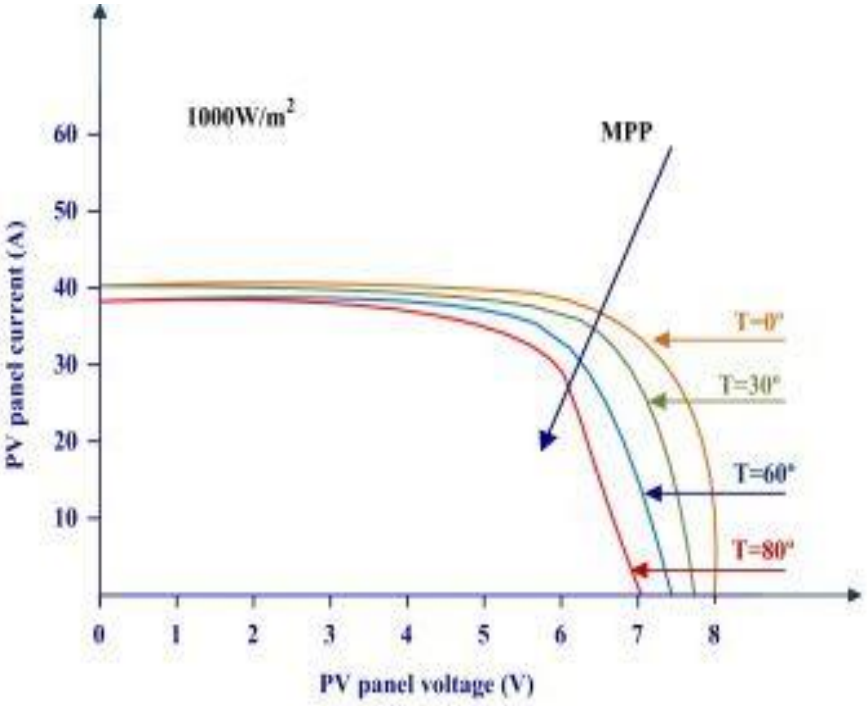

Figure 2.3 I–V characteristic at constant insolation and different temperatures.

The photo current I_{ph} and hence the PV panel short circuit current depends on the irradiation and temperature as given in Figure 2.4 and 2.5 which implies as radiations increases, the current and hence power increases. The open circuit voltage increases logarithmically with the incident irradiation, while the short circuit current is a linear function of the incident irradiation.

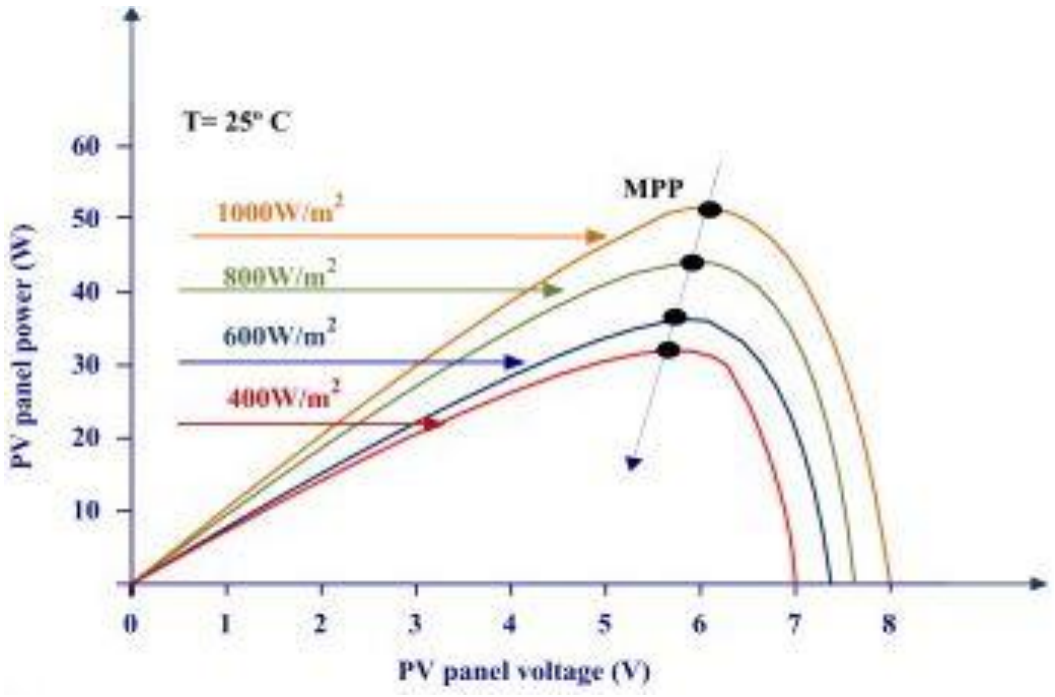

Figure 2.4 P–V characteristics at constant temperature and different irradiations.

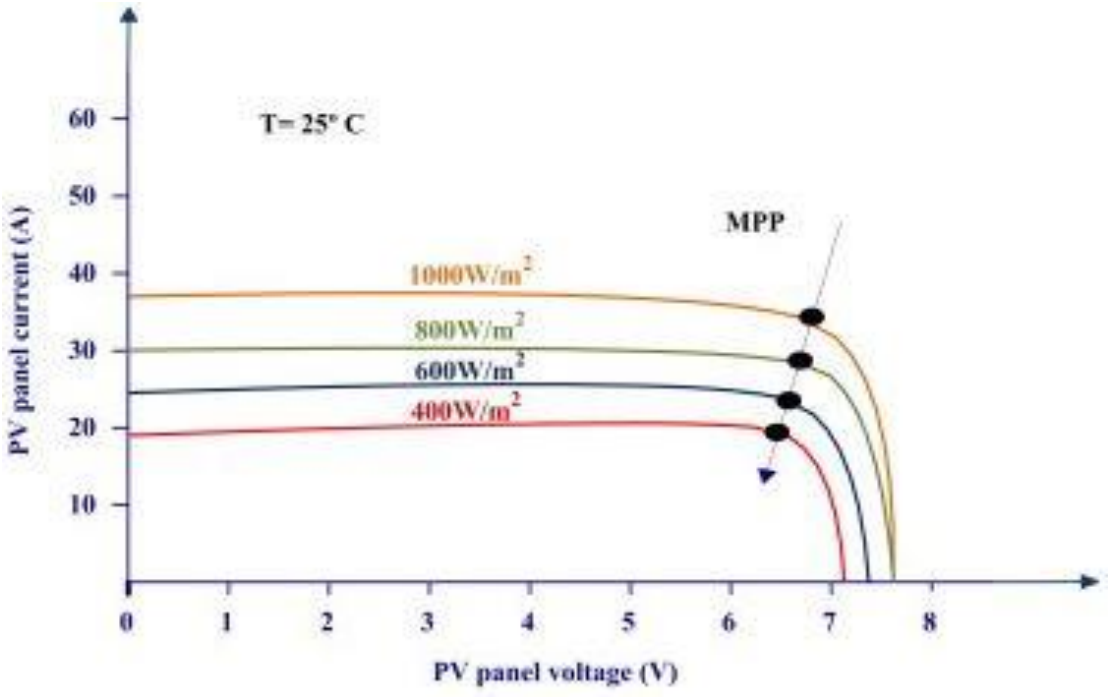

Figure 2.5 I–V characteristics at constant temperature and different irradiations.

2.4 Maximum Power Point Tracking Techniques

Due to changing environmental conditions the characteristics of the photovoltaic array changes and the maximum power point varies. It is desired to obtain maximum power under all environmental conditions and hence it is important to track the maximum power point. The techniques by which the maximum power point is tracked on the P-V characteristics of the photovoltaic panel to accurately determine the MPP under varying environmental conditions are known as maximum power point tracking techniques (MPPT) [1]. Electrical tracking (MPPT) is a process in which *I–V* curve of the panel is tracked for MPP. Usually power electronics devices are used in renewable energy systems to track the MPP. The MPP is tracked in order to harness maximum power and achieve maximum efficiency.

There are various ways to classify MPPT techniques, some depend on the number of variables used to track MPP like one variable or two variable methods, and some based on the type of techniques used to track MPP. The most commonly used MPPT control techniques are:

2.4.1 Voltage (open-circuit) based MPPT

The open circuit voltage V_{OC} and maximum power point voltage V_{MPP} have a linear relation for different solar irradiation and operating temperatures. This is used to develop voltage MPPT technique. Equation 2.7 gives relation between V_{MPP} and V_{OC}.

$$V_{MPP} \cong K_{mv} V_{OC} \tag{2.7}$$

Where K_{mv} is called *voltage factor* and its value varies from 0.7 to 0.95 depending upon the characteristics of the PV panel. In this method, a switch has to be connected in series with the converter and the panel, the open circuit voltage is measured across this switch while it is off. The MPPT sets the PV array current to zero for a very short period by opening the circuit and measure V_{OC} then V_{MPP} is calculated according to Equation 2.7. The MPPT controller then, changes the duty cycle to obtain load voltage equals to V_{MPP}. This process is repeated periodically to get maximum power. Since sensors required are less and no derivatives are required to be calculated it is a practical method for MPP estimation [12]. The major disadvantage of this technique is the loss of power during sampling of open circuit voltage. The pros of this method is that it uses only one feedback loop and it is economic and simple.

2.4.2 The Perturb and Observe Method

This is an iterative method of MPPT tracking. It is also known as the "hill climbing" algorithm. It regularly sense the panel working voltage and calculate PV output power with the previous comparison, the operating voltage is changed by the duty cycle and the change in the direction of power is observed to track MPP. The sign of change in power is determined, if the power is increased by increasing the voltage then the operating voltage is further perturbed in the same direction as shown in Figure 2.6, this process continues till $dP/dV=0$. Once the MPP is reached, the voltage still oscillates around the MPP, instead of being stable on it, as voltage is perturbed at MPP also. This is one of the biggest disadvantages of this method [13]. Also, due to periodic perturbations in voltage there is significant amount of power loss in this method. In rapidly changing environmental conditions this method doesn't provide appropriate results, also this method is slow in tracking the MPP as it takes several steps. The advantage of this method is it does not require panel characteristics so it can be employed for any solar panel.

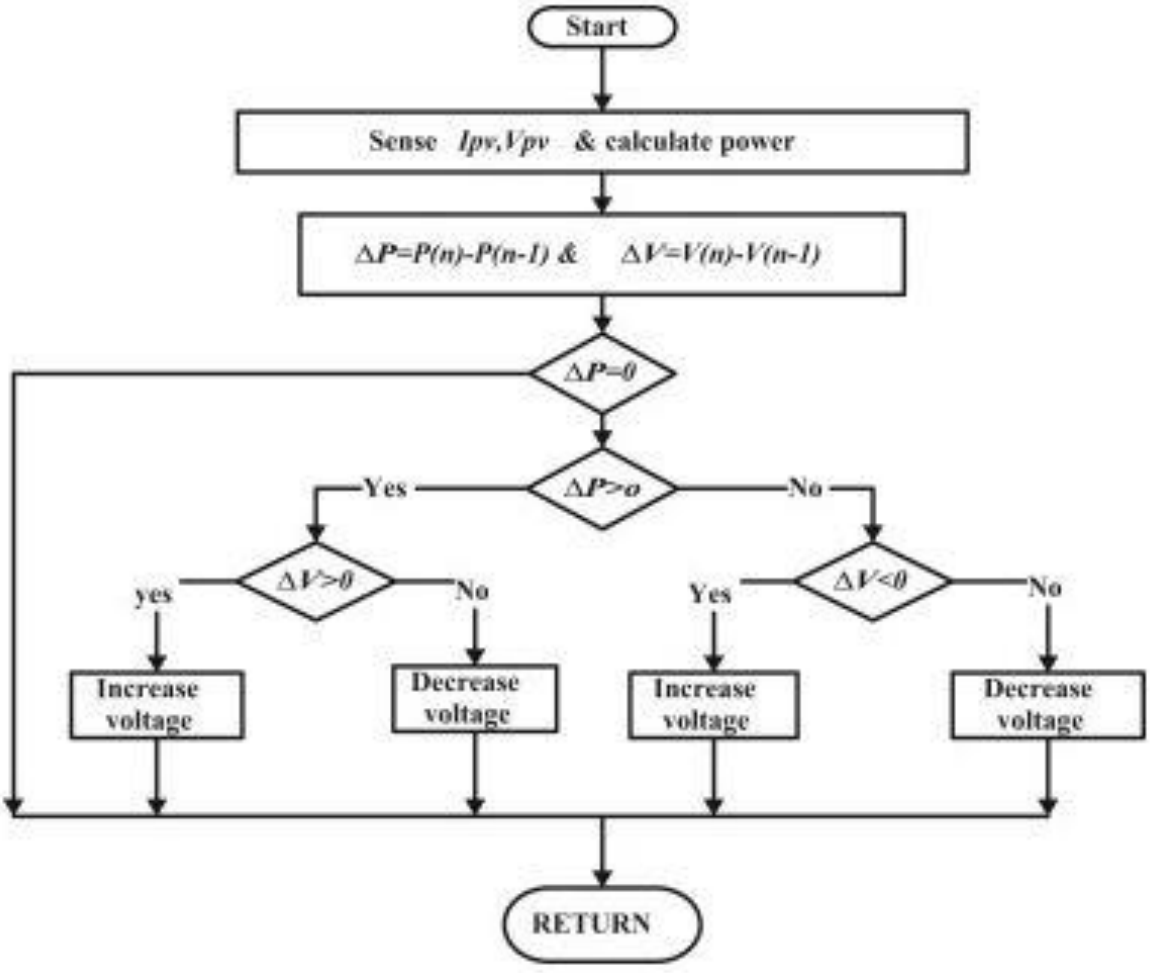

Figure 2.6 Flow chart of P&O algorithm.

2.4.3 Incremental Conductance Method

Incremental conductance method is a very extensively used MPPT technique. The drawbacks of P&O method, of oscillation of operating point around MPP during changing environmental conditions can be overcome in INC method by comparing the instantaneous panel conductance (I_{PV}/V_{PV}) with the incremental panel conductance (dI_{PV}/dV_{PV}). The voltage of MPP is tracked to satisfy $dP_{PV}/dV_{PV}=0$, which is MPP. INC based algorithm is better than other conventional methods because it is easy to implement, provides high tracking speed and better efficiency. Present and previous values of the photovoltaic panel voltage and current are sensed in this algorithm and are used to calculate the values of dI_{PV} and dV_{PV}. The algorithm is as shown in Figure 2.7, for current based incremental conductance MPPT, similar algorithm exists for voltage based control where voltage is sensed compared and changed.

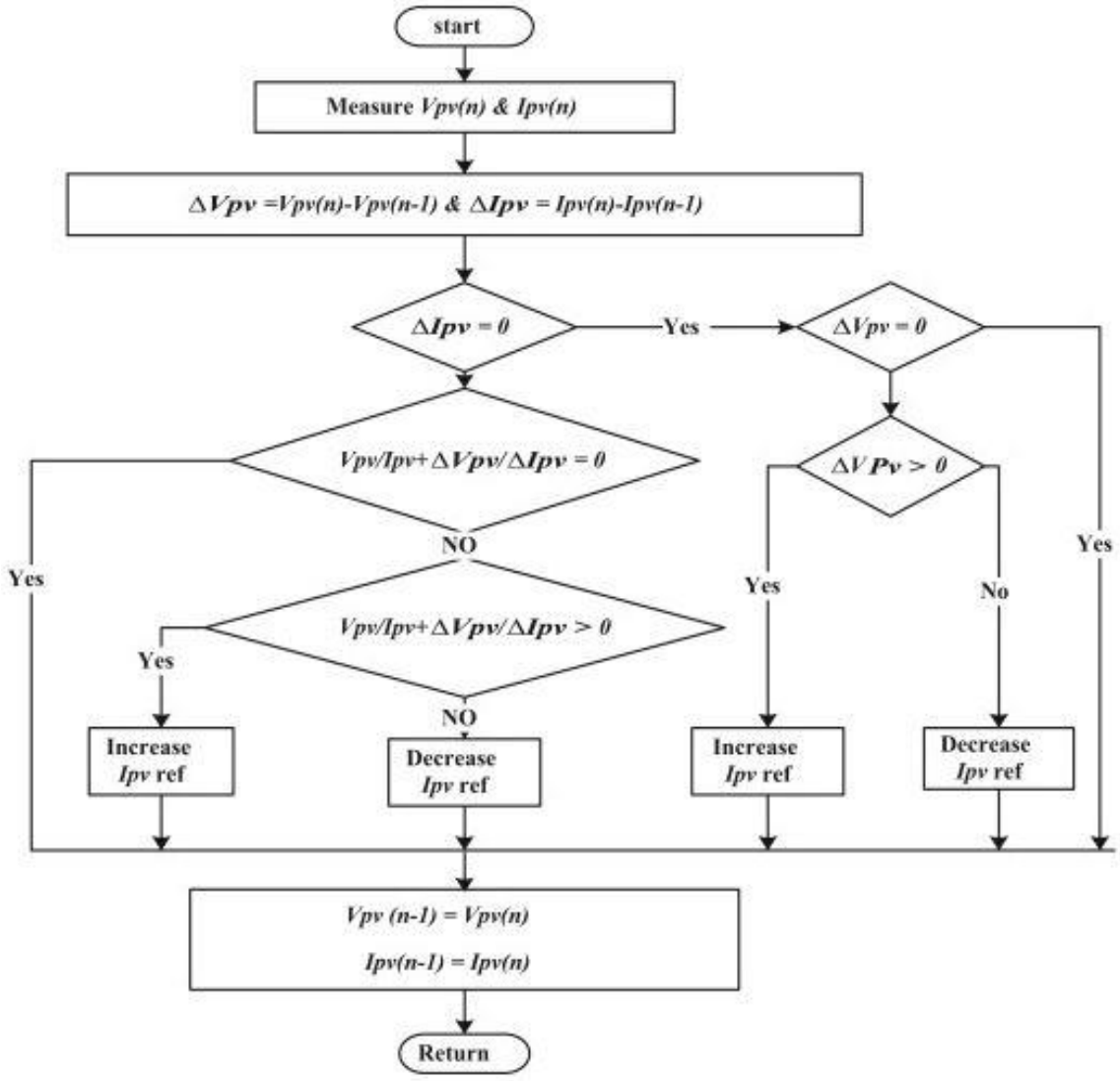

Figure 2.7 Flow chart of Incremental conductance method.

CHAPTER 3: MULTIPORT CONVERTERS

3.1 Introduction to Multi-port Converters

A power electronic system, as shown in Figure 3.1, usually consists of a load, an energy source, a switching converter and a control circuit. The key component is the switching converter, which proficiently processes the power from its available input form to the desired output form according to the signal generated by the control circuit. The switching converter is also known as a two-port converter since it has two power ports, one port is connected to the input which is usually the source and other is connected to the load.

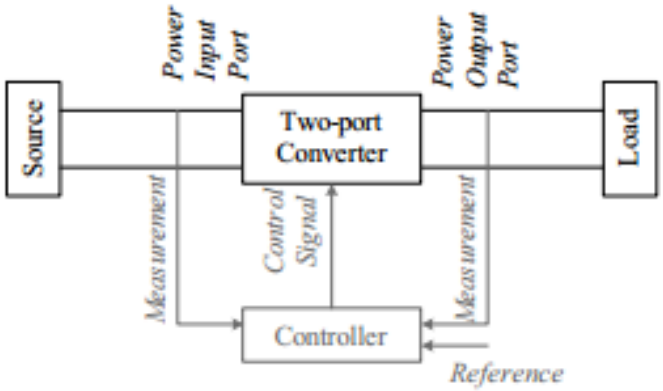

Figure 3.1 Block diagram of a two port power converter system.

However, there are also some special cases, i.e. a system may accommodate multiple sources and/or multiple loads. The assembly of such a system mostly includes an intermediate power bus and is configured using several two-port converters to interconnect the bus and the sources/loads, as illustrated in Figure 3.2. These two-port converters are independently controlled and a communication bus may be required for the purpose of managing power flow. The main disadvantage of this assembly is the complexity of the whole system, even if every two-port converter is simple and realized with the minimum number of power switches.

A multi-port converter, i.e. a single power processing stage with multiple power ports, as illustrated in Figure 3.3, is emerging because it offers an opportunity to make the whole system simpler and more compact [15]. Thus multi-port converter cannot only interface all sources/loads, and modify the electrical energy form, but also manage the power flow between the sources and the loads.

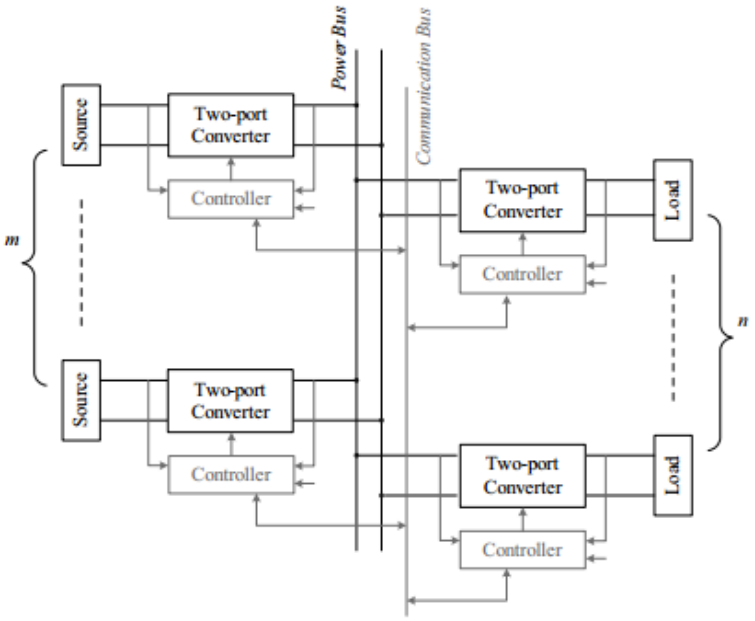

Figure 3.2 Block diagram of a power electronic system with several two-port converters.

The major advantage of the multi-port converter over various two-port converters with an intermediate power bus is that less power switches, less associated gate drivers and less passive components are needed since the partial redundant power processing units in the two-port converters are eliminated [8]. Thus cost can be reduced, and higher power efficiency and higher power density can be achieved. Moreover, better dynamic performance can be obtained since the communication time between the different control circuits for the two-port converters does not exist anymore due to the centralized control.

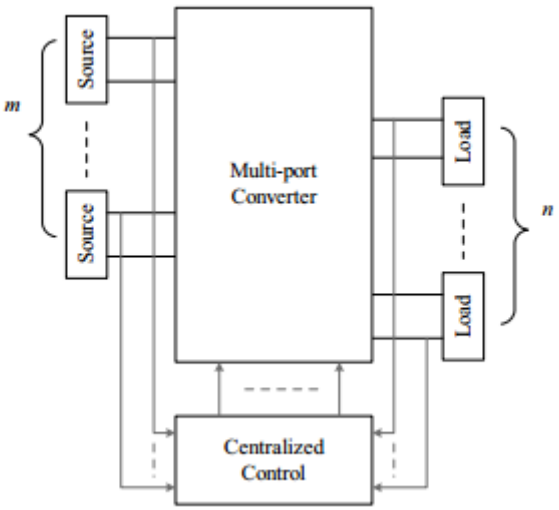

Figure 3.3 Block diagram of Multi-port Converter.

3.2 Advantages of Multi-port Converters

The multi-port converters are in demand because of their potential application in renewable energy generation systems, hybrid electric vehicles (HEVs), uninterruptible power supplies, fuel cell vehicles (FCVs), and any other application with the requirement to interface multiple sources/loads. The motivation to use multi-port converters, the assembly and basic function of the systems are discussed in following energy management applications: a renewable energy generation system, a misbalanced voltage electrical system in HEVs and FCVs.

The major advantage of the multiport converter over two port converter with an intermediate energy bus is that fewer power switches, controllers and passive components are required. The potential applications of multi-port converter is in the electric voltage systems, hybrid electric vehicles and fuel-cell vehicles [3]. Multiport converters have multiple input and/or output and bi-directional ports where energy sources and electric loads can be connected.

The role of the converter is to manage the power flow between the sources and loads. All the ports possess the ability of bidirectional power flow. A multiport converter can manage the simultaneous power flow from any number of ports and the voltage of various ports can be at different levels ranging from dozens to few hundreds. In order to make the efficient use of energy storage system it should be connected to a bidirectional port. In general, all ports are considered to be bidirectional. Therefore, it is not required to distinguish the ports as input or output. This is the reason why the converter is called a multiport converter instead of a multi-input or multi-output converter. Therefore both load and source can act interchangeably.

3.3 Multi-port Converter Topologies

3.3.1 DC-linked three-port converter

Few general three-port converter topologies are presents in this section which are broadly used depending upon the power requirements. A three-port converter topology is employed to interconnect a renewable source (fuel cell), a storage unit and a load. The converter topology shown in the figure below uses a DC link to connect the ports. There are various methods to create such a converter. Figure 3.4 shows a converter which links the DC bus with the fuel cell, storage and load [6]. This is the simplest structure and it finds a potential application in hybrid vehicles where a high voltage renewable source is connected to a storage and the difference in voltage level is very high. Since all the switching cells are directly

connected in parallel, any standard switch module can be applied (e.g. a three-phase bridge module for four-port applications, or a full-bridge module).

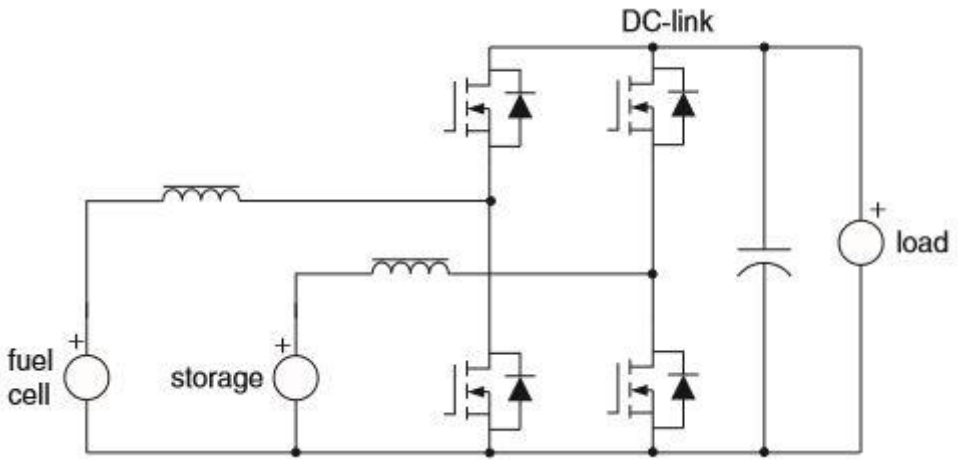

Figure 3.4 DC-linked three-port converter.

3.3.2 Magnetically coupled three-port converter

Figure 3.5 shows a three-port converter (the triple-active-bridge converter) which is magnetically coupled. Full bridges can be used in place of the half bridges. The main advantages of this converter is, it provides galvanic isolation and voltage levels of various ports can be matched comfortably by choosing the suitable number of turns for the windings. The resulting leakage inductances will be an integral part of the circuit as energy transfer elements. The dual-active bridge (DAB) converter is extended to create this converter. A phase shift angle controlled high frequency voltage (square wave in the easiest case) is generated by each bridge. The voltages applied to the windings possess the same frequency. The phase shift control the power flow in the three ports. Provided the operating voltage is constant at each port this converter can be controlled by soft switching [14]. However, in the cases when operating voltage varies widely, such as supercapacitors, the operating range of soft-switching will be reduced. A method has been proposed to increase the range of soft-switching by controlling the duty cycle of the voltage applied to the winding (rectangular-pulse wave) according to the port DC voltage. The control scheme of the converter topology has been discussed in the following sections.

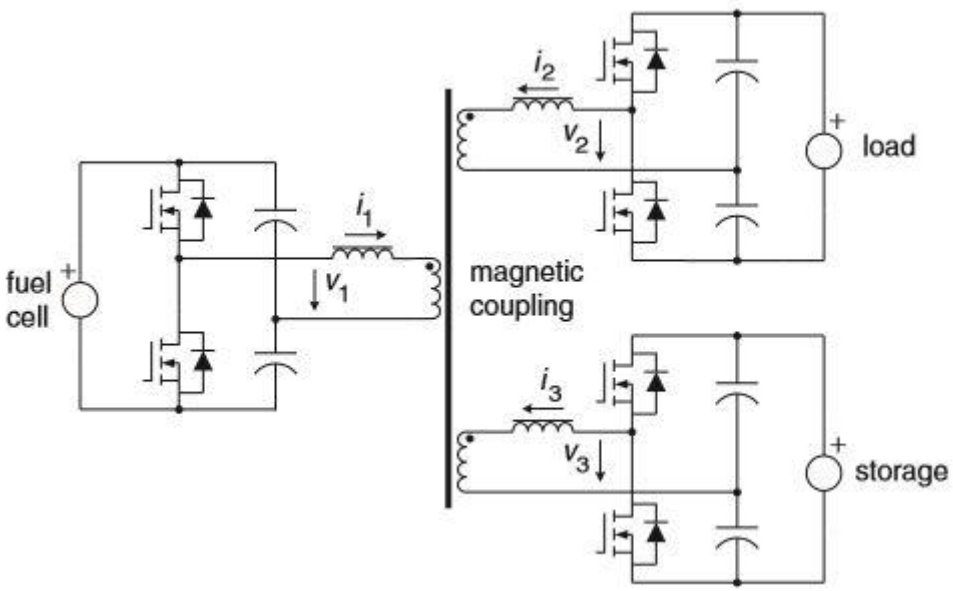

Figure 3.5 Magnetically coupled three-port converter.

3.3.3 Three-port converter combining DC-link and magnetic coupling

A converter combining a DC-link and magnetic coupling is illustrated in Figure 3.6. The renewable energy source (fuel cell) and the storage battery are connected via a DC bus link in this converter as the voltage difference between them is less, and the load is integrated through a transformer winding . This three-port bidirectional converter topology consists of six switches. This converter topology is employed in the applications where the sources are operating at low voltages which needs to be stepped up to supply the load. , e.g. 400V. This topology can also be used to supply an AC load.

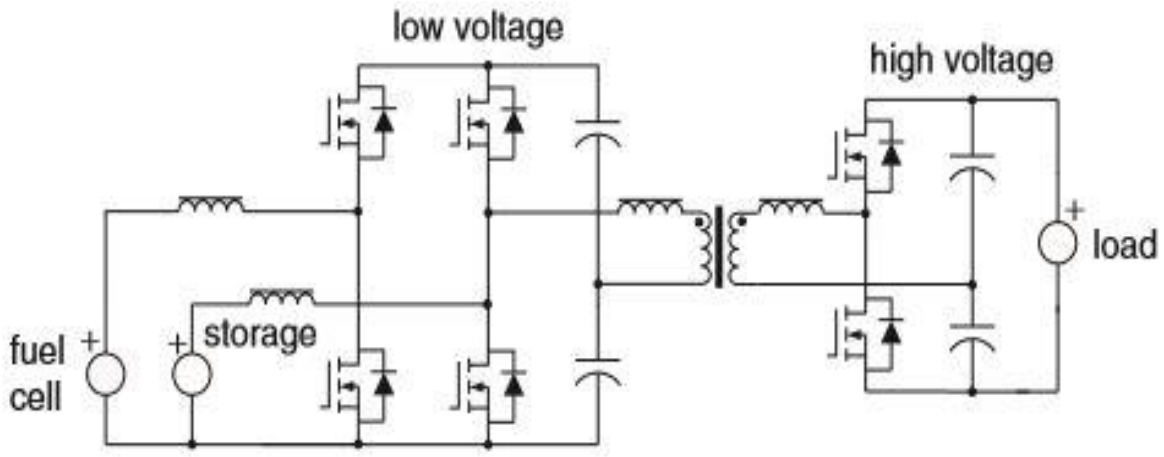

Figure 3.6 Three-port converter combining DC-link and magnetic coupling.

3.4 Control Strategy

Various topologies has been discussed in detail so far. A multi-port converter is able to manage the power flow between various source and load with the help of a well refined control strategy. Figure 3.7 shows the control system of a multiport converter which is a usual multi-input multi-output (MIMO) condition, where the parameters that need to be controlled can be output voltages, source currents (e.g. fuel cell current), source powers (e.g. maximum power point tracking of a PV) etc. The phase shifts and duty cycles are the system control variables.

The theoretical control scheme is shown in Figure 3.7. Suppose there are N sources that are being connected using the magnetic coupling, whereas DC link is used to couple M sources. Therefore there are in total N+M independent control variables (N phase shifts for magnetic coupled and M duty cycles for DC linked). PID/PI controller is used to compute each control variable. Circuit parameters like voltage and current are sampled in real time using sampling circuit, to compute the objective variable that are hard to sample, for example power [18]. Power flow management unit generates the reference signals to compare them with the output of sampling circuit. In response to certain operating conditions, the reference signals are calculated by the power flow manager, for example the state of charge (SOC) of the storage element. The phase shift generator is used to generate phase-shifted square waves (PSSW) for the magnetically coupled sources and the PWM generator is used to generate the pulse-width modulation (PWM) signals for the DC linked sources.

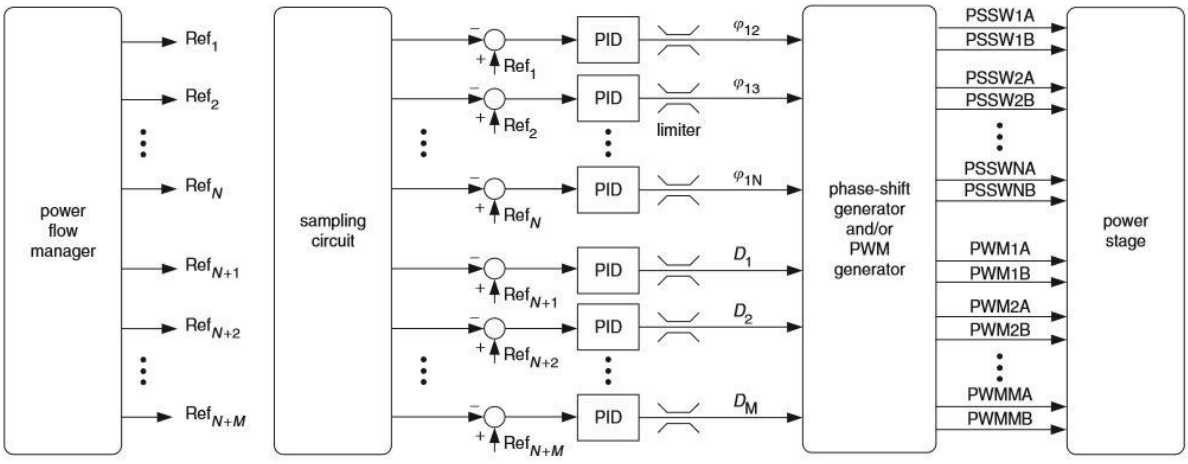

Figure 3.7 Control strategy of multiport bidirectional converter.

CHAPTER 4: THREE-PORT CONVERTER TOPOLOGY AND OPERATION

4.1 Converter Details and Circuit

Figure 4.1 shows a Three-port converter which comprises of two DC/DC converters. The Buck converter is unidirectional, which is controlled by the Maximum power point tracking (MPPT) control to extract the maximum power from the photovoltaic array. A 12V battery is connected to the DC bus in parallel via a bidirectional DC-DC converter to allow power flow in both directions. This system can power both DC and AC by employing DC/DC or DC/AC converter respectively at the load port. DC bus can power the load directly if the load voltage and DC bus voltage are same.

The bi-directional DC/DC converter plays an important role in the system by transmitting energy in both directions [16]. The major advantages of bidirectional Buck/Boost converter are that it is easy to configure, simple control and it has a fast response. Additionally it can limit the current through battery to prevent any damage. Power diode of the traditional Buck DC/DC converter is replaced by power MOSFET to develop the bidirectional DC/DC converter [20]. MOSFET Q1 is controlled to operate in Buck mode while MOSFET Q2 is controlled to operate in Boost mode.

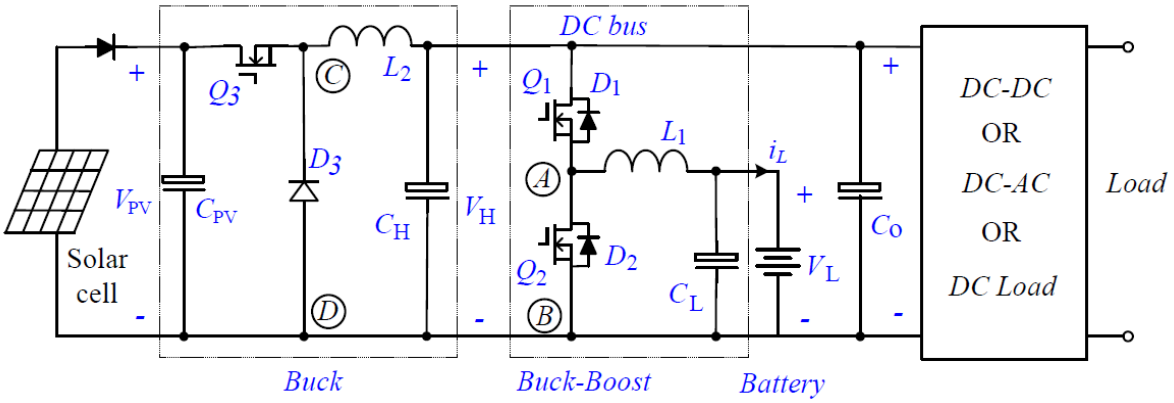

Figure 4.1 Three-port converter topology.

The operation of the system in Figure 4.1 can be explained easily by its energy flow model, as shown in Figure 4.2. When photovoltaic panel can produce more power than needed by load ($P_{pv} > P_o$), solar cell will power the load and the remaining power will charge the

battery, bidirectional DC/DC converter will operate in buck mode and the energy will flow into the battery, as shown in Figure 4.2(a). Especially, when there is no load (P_o=0), bi-directional DC/DC converter will operate in buck mode and will charge the battery [4]. When solar cell cannot produce enough energy to power the load ($P_{pv} < P_o$), battery will supplement the solar to power the load. Bi-directional DC/DC converter will operate in boost mode and will discharge the battery, as shown in Figure 4.2(b). Especially, when the output power of solar cell is zero (P_{pv}=0) in the conditions like overcast sky or at night, solar will not be able to power the load so the battery will power the load via the bi-directional DC/DC converter operating in boost mode.

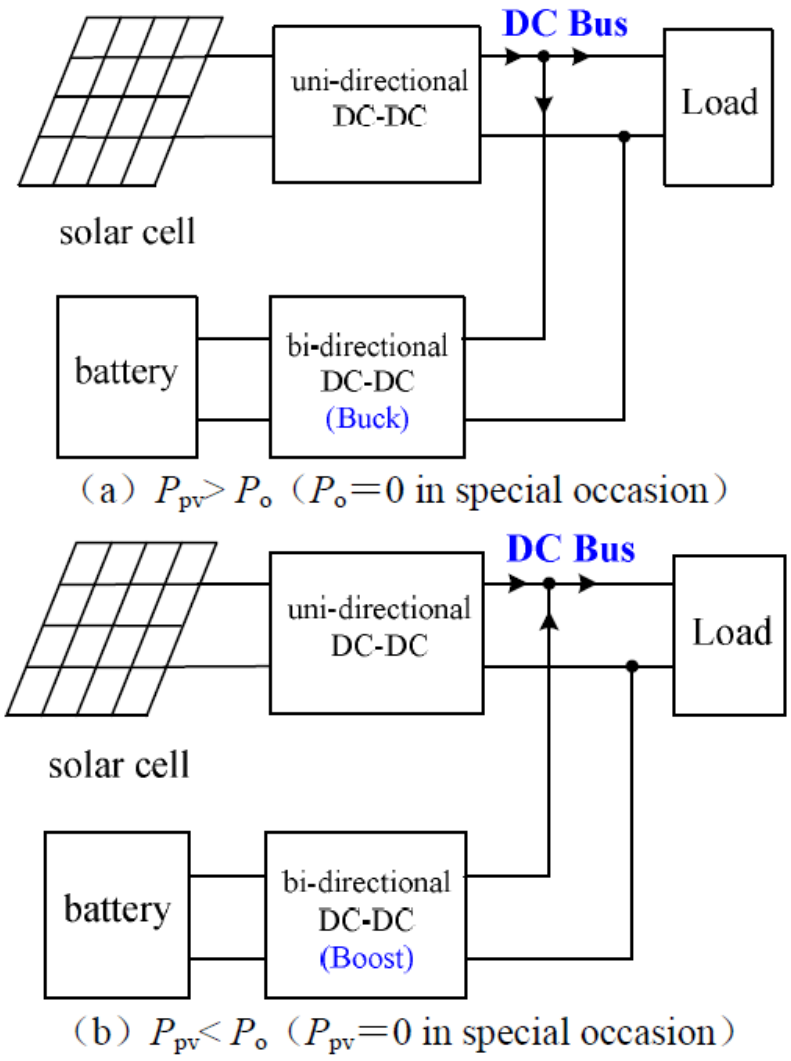

Figure 4.2 Power flow depending upon PV array power and Load power.

4.2 Control Strategy

4.2.1 Control of Buck Converter

It is always desired to attain Maximum Power output at minimum cost under various operating conditions. However, the Maximum Power Point differs with solar irradiation. Maximum power point is difficult to achieve at different solar irradiations. Hence, Maximum Power Point Tracking algorithm (Perturb and Observe method) is used with buck converter [2]. The PWM pulses generated for the duty cycle obtained from perturb and observe algorithm is supplied to the buck converter.

When the battery is fully charged and the photovoltaic cell is supplying more power than load then the buck converter will be controlled by the PI controller, which maintains a constant DC bus voltage. Since battery is fully charged and cannot absorb energy, the DC bus voltage will rise if MPPT algorithm is used hence, instead of extracting maximum power only desired power is extracted to maintain a constant DC voltage.

4.2.2 Control of Bi-directional converter

The proposed battery charger algorithm shown in Figure 2.4, checks the DC bus voltage and the battery state of charge (SOC). Depending upon these system parameters, the controller selects the operating mode of the bidirectional converter. Rapid response is desired from the controller to maintain the balanced power flow among all the ports. When the battery state of charge (SOC) is in between 10% and 90% and the voltage of the DC bus falls below 24 V then the bidirectional converter operates in Boost mode and supplement the solar power to maintain a constant 24 V at the DC bus [7]. Similarly when the voltage start rising above 24 V the bidirectional converter starts operating in Buck mode and charge the battery. If the battery SOC falls below 10% or rises above 90 % then the bidirectional converter enters the halt mode to prevent the deep discharge or overcharging of the battery respectively. The overall control of the bidirectional converter is divided into three mode charging, discharging and halt. Bidirectional converter plays an important role in maintaining the steady power flow among photovoltaic panel, battery and the load.

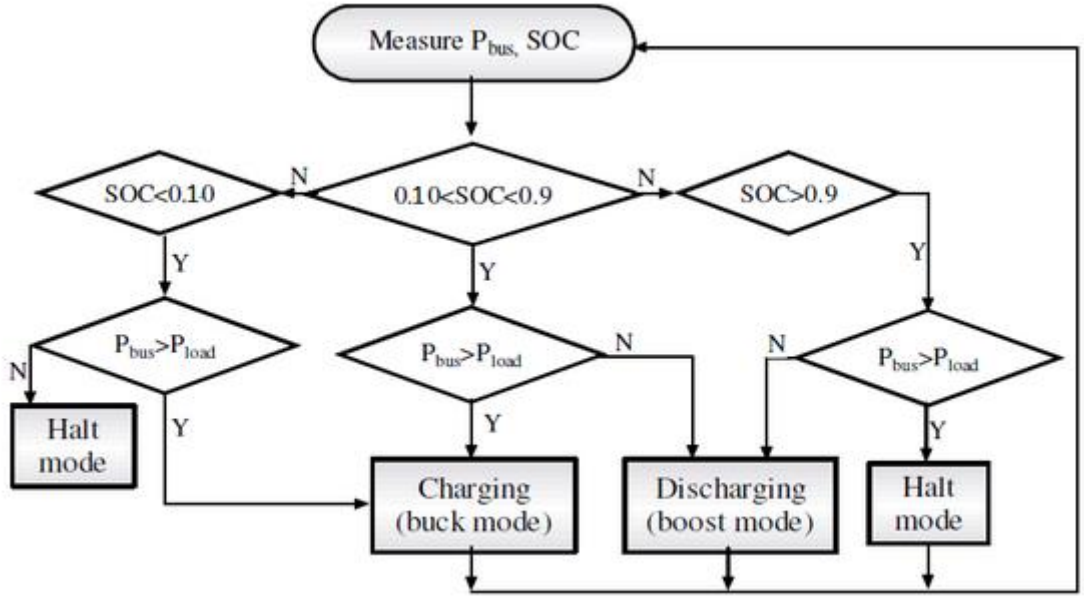

Figure 4.3 Bi-directional converter control Algorithm.

4.2.3 Control of DC Motor Drive

Separately excited DC motor is being controlled to operate in 1st and 2nd quadrant i.e. forward motoring and forward generating mode. A two-quadrant chopper has been used to operate the motor in regenerative braking mode. A two-quadrant chopper consist of a halt-bridge which comprises of two switches and two diodes [26]. As shown in Figure 4.4 complementary PWM signals are given to both the switches to operate the machine in forward motoring and regenerative braking mode.

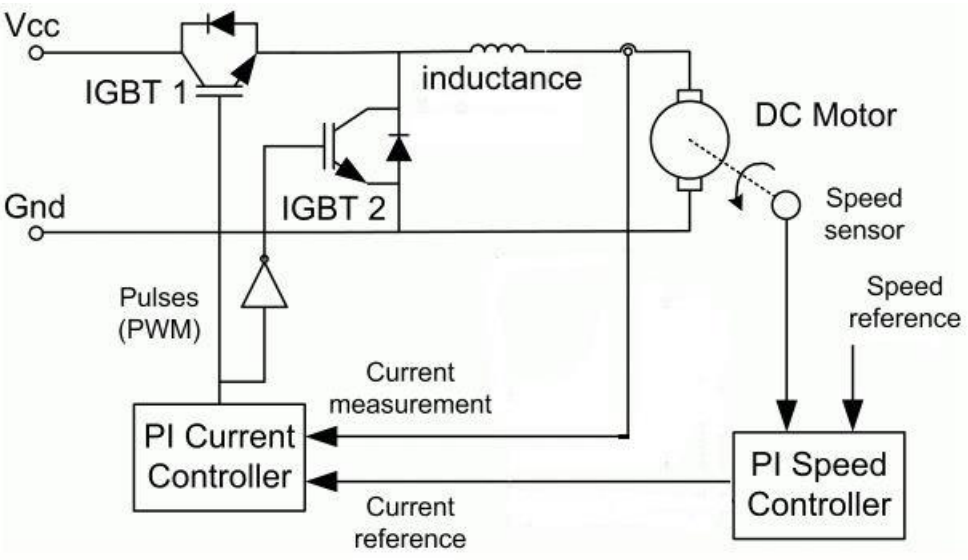

Figure 4.4 Two quadrant chopper control circuit.

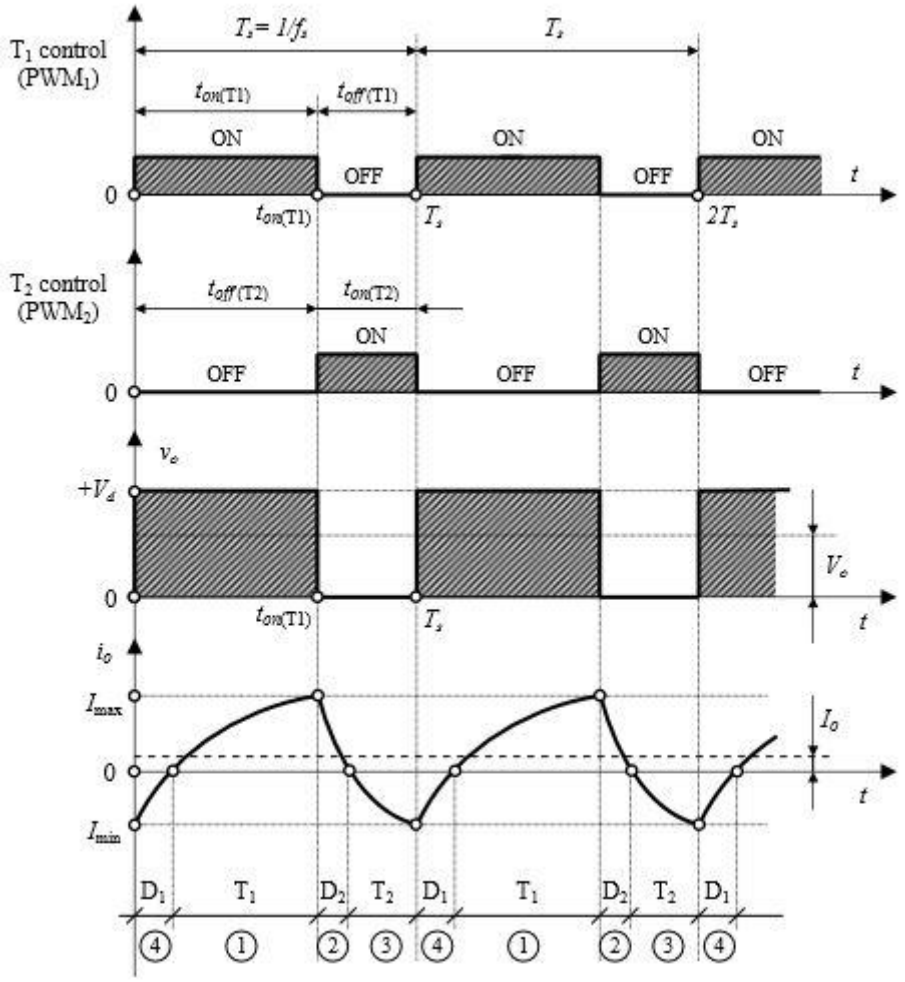

Figure 4.5 Control pulses of Two-quadrant chopper.

In the region marked 1 in Figure 4.5 IGBT1 will be switched ON and the motor will operate in forward motoring mode, during this period IGBT2 will be OFF. After T1 time IGBT2 will be switched ON but the inductor is charged so it will continue to flow the current in same direction via body diode of IGBT2 until it discharges. In the region marked 3 the motor will start to deaccelerate as the inductor will be charged during this period via IGBT2 [25]. After time T1 + T2, IGBT1 will be switched ON again but as the inductor is charged it will flow the current in negative direction only and will supply power to the source. During the region marked as 1 and 2 the motor will be in forward motoring mode while in regions marked as 3 and 4 the will be in regenerative braking mode and will supply power to the source.

CHAPTER 5: SIMULATION CIRCUIT AND RESULTS

5.1 Simulation Circuit

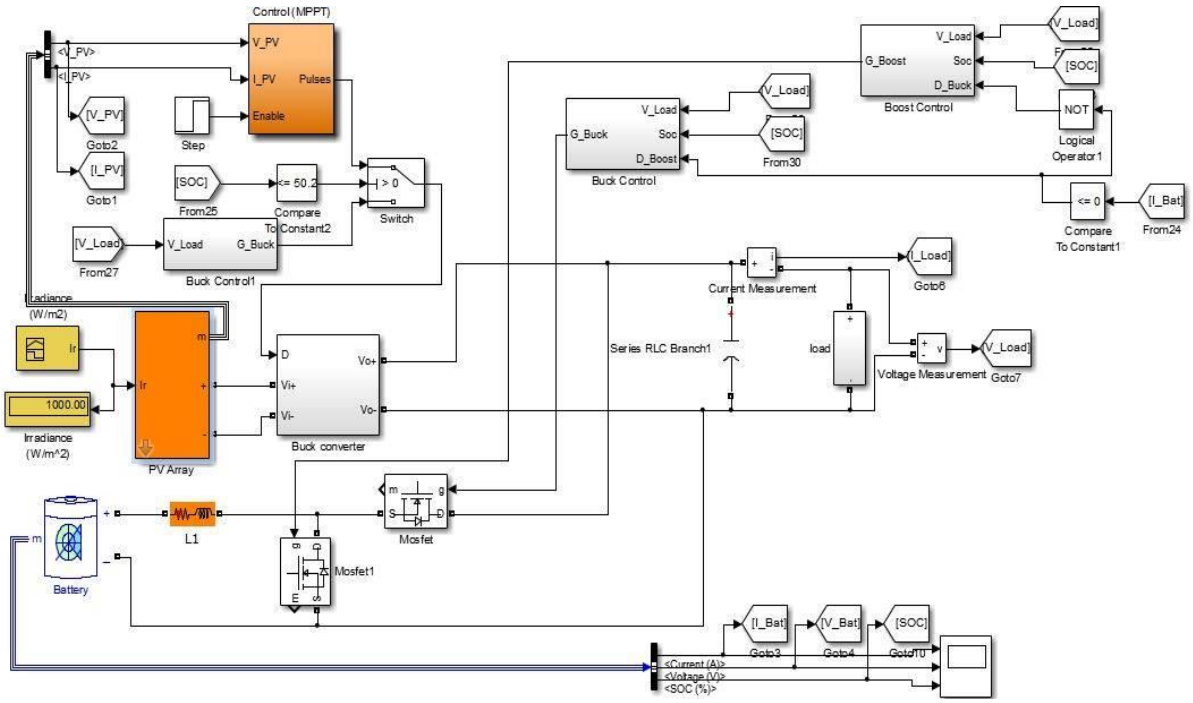

Figure 5.1 Simulation circuit.

Simulation circuit shown in Figure 3.1, consists of a Photovoltaic array connected to the buck converter at port 1. Buck converter is used to step-down the PV array voltage (26 V – 33 V) to 24 V. PV array block takes irradiance as input, maximum power supplied by the PV array depends on the irradiance. MPPT control block is used to generate the firing pulses for the buck converter connected to the PV array. This MPPT control block is enabled at T = 0.1 s. MPPT control block takes PV array current and voltage as input. Switch connected to MPPT control block switches to PI control block when the battery is fully charged according to the control strategy described in the previous section.

A 12 V Battery is connected at port 2 via a bi-directional DC-DC converter. Switching signal for the battery charging MOSFET is generated by Buck control block. Buck control block consists of a closed loop PI controller which takes DC bus voltage as input and operates when battery is not fully charged and battery current is negative. Switching signal for the battery discharging MOSFET1 is generated by Boost control block. Boost control block also

consists of a closed loop PI controller which takes DC bus voltage as input and operates when battery is not fully discharged and battery current is positive. Load block consists of a variable resistor and is connected to the DC bus which has a constant voltage of 24 V. Load is connected at port 3.

5.2 Parameter Calculation

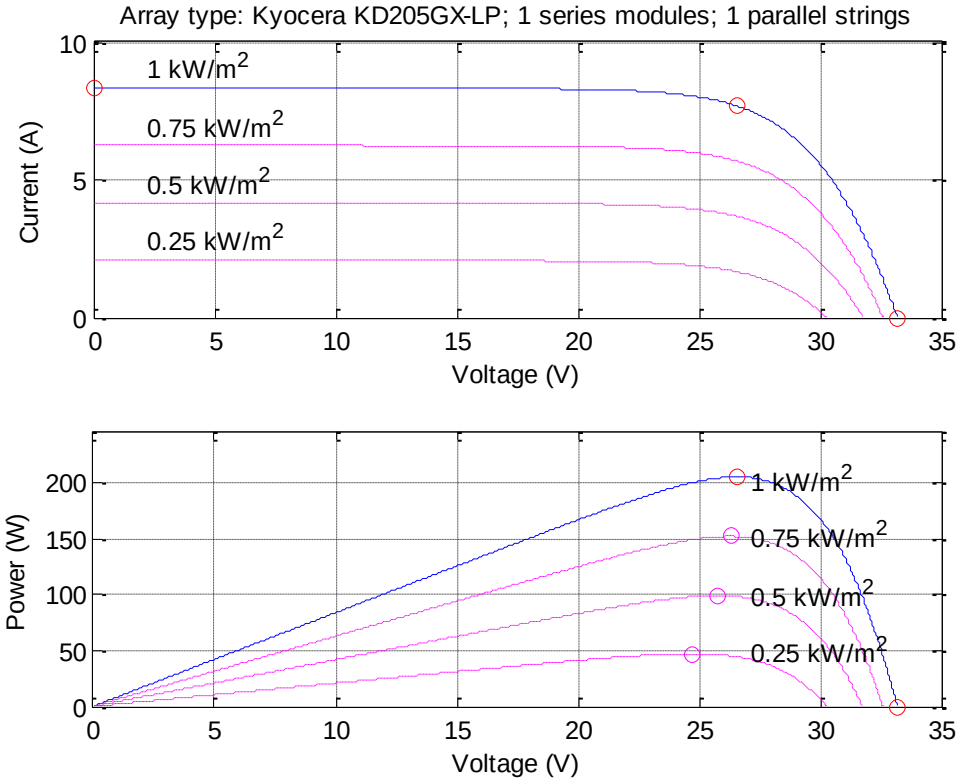

Figure 5.2 PV Array characteristics.

V_{oc}	33.2 V
I_{sc}	8.36 A
V_{mp}	26.6 V
I_{mp}	7.7 A
P_{max} (@1000 Ir)	210 W
P_{max} (@700 Ir)	150 W
P_{max} (@200 Ir)	30 W
P_{max} (@100 Ir)	10 W

Table 5.1 PV Array Parameters.

For Buck converter (continuous mode)

$$L_{\min} = \frac{(1-D)R}{2f} \tag{5.1}$$

$$C = \frac{1-D}{8L\left(\Delta V_0 / V_0\right) f^2} \tag{5.2}$$

For Boost converter (continuous mode)

$$L_{\min} = \frac{D(1-D)^2 R}{2f} \tag{5.3}$$

$$C = \frac{D}{R\left(\Delta V_0 / V_0\right) f} \tag{5.4}$$

D is the duty cycle of the converter,

f is the operating frequency of the converter,

$L_{\min}$ is the minimum inductor required for continuous mode,

C is the minimum capacitor required for continuous mode,

$\left(\Delta V_0 / V_0\right)$ is the acceptable ripple voltage,

R is the resistance of load.

L_{Buck}	$5*10^{-4}$ H
C_{Buck}	$10*10^{-4}$ F
$L_{Bi\text{-}di}$	$5*10^{-4}$ H
$C_{DC\ bus}$	$40*10^{-4}$ F
MPPT Enable	0.1 s
DC bus Voltage	24 V
Full charge condition	50.2 %

Table 5.2 Circuit Parameters.

5.3 Simulation Results

5.3.1 Variable Irradiance (Load = 8Ω)

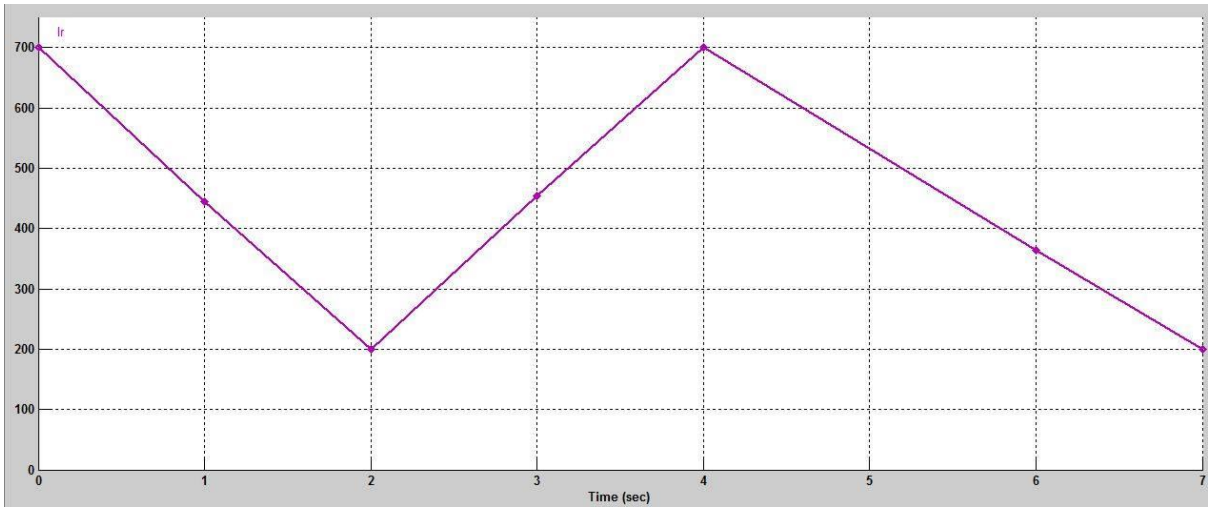

Figure 5.3 Variable Irradiance (200W/m^2 – 700W/m^2).

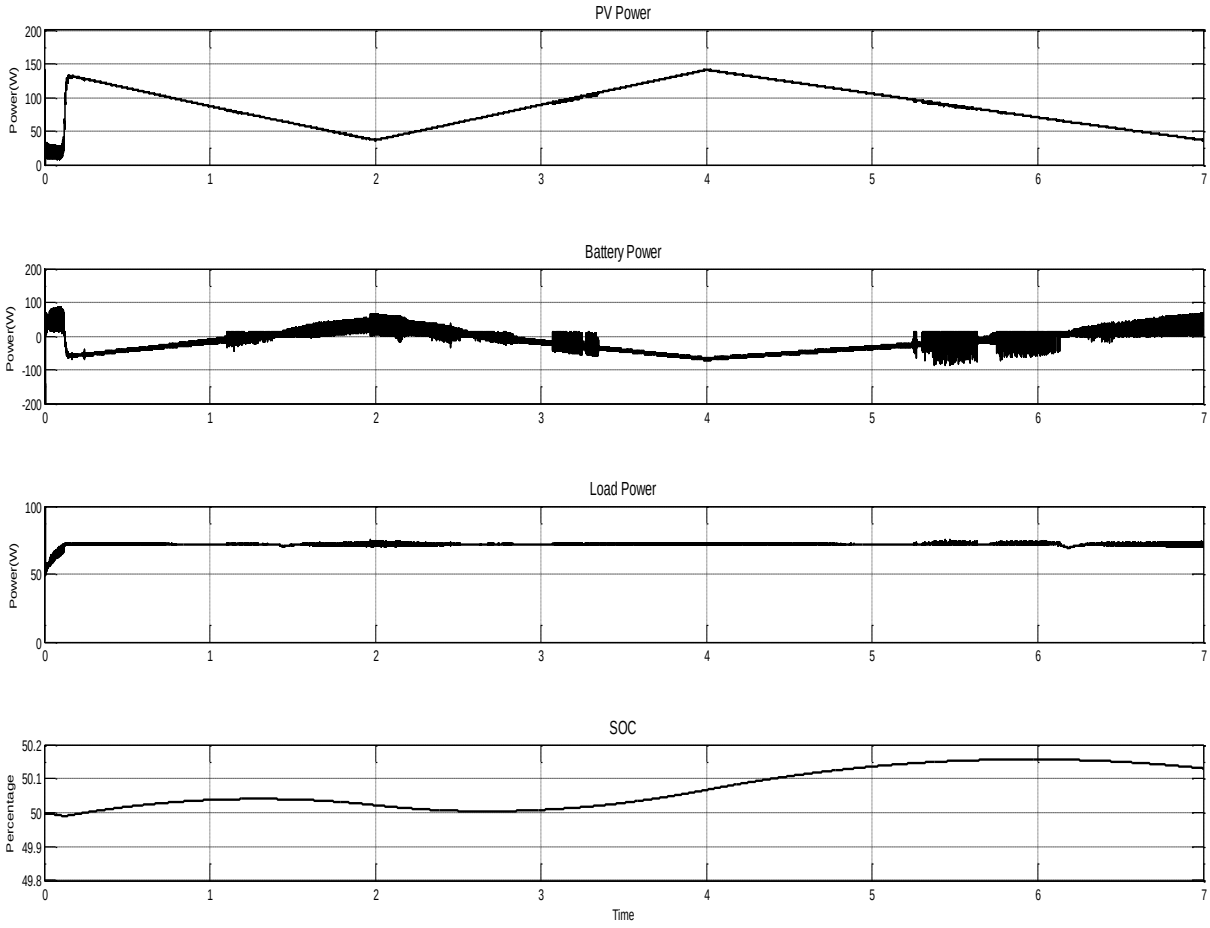

Figure 5.4 Power and SOC waveforms corresponding to variable irradiation.

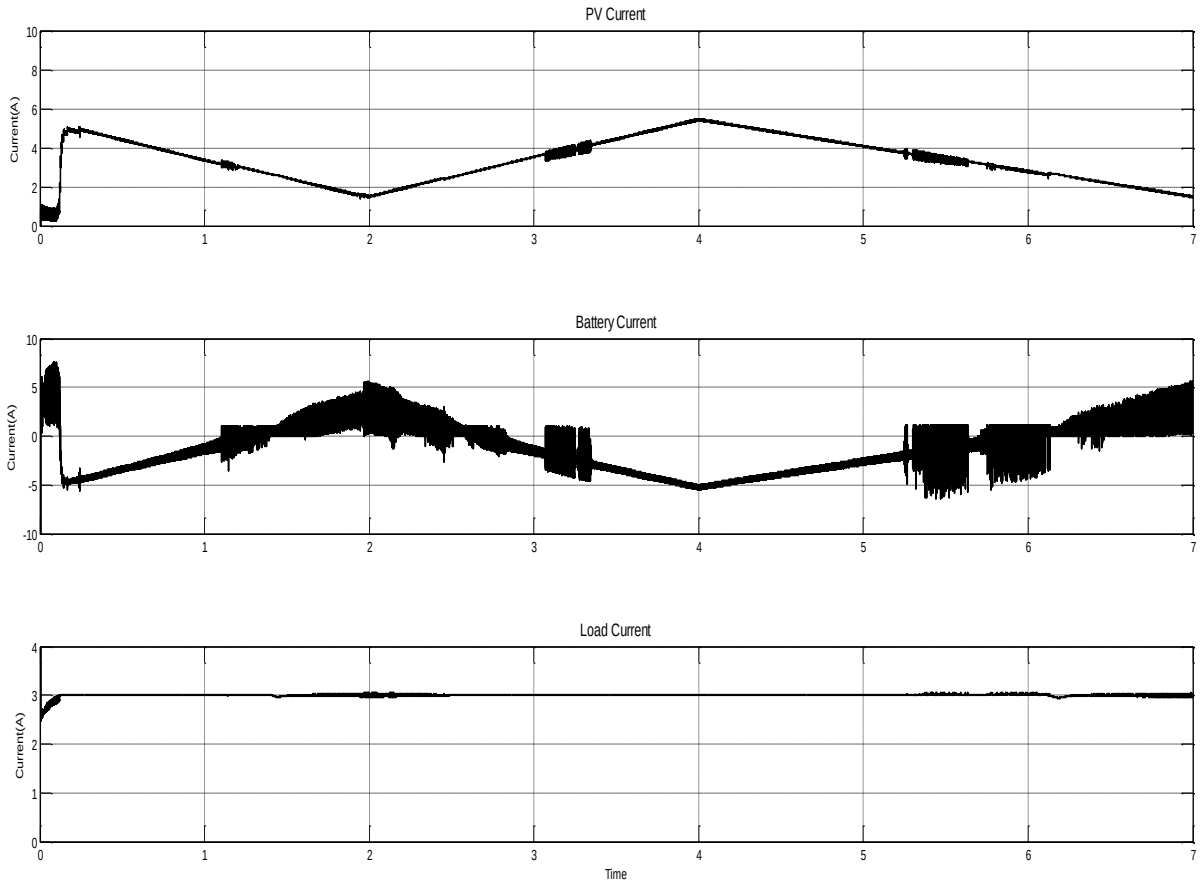

Figure 5.5 Current waveforms corresponding to variable irradiation.

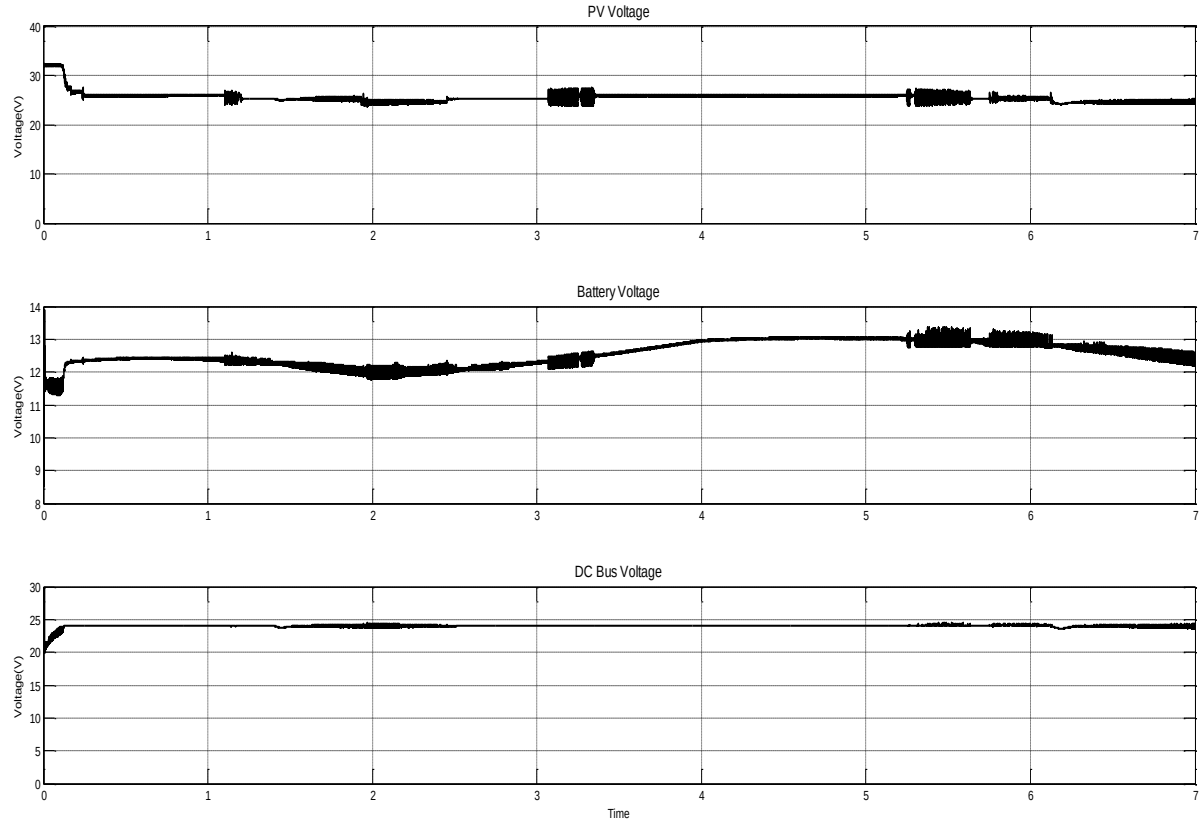

Figure 5.6 Voltage waveforms corresponding to variable irradiation.

A resistive load is connected at port 3 directly across the DC bus. The power produced by the photovoltaic panel will vary as the irradiation is varying from 200W/m^2 – 700W/m^2 as shown in Figure 5.3. A 12 V battery is connected at port 2 via a bidirectional DC-DC converter.

Since the load is constant, a constant amount of power will be drawn by the load. Change in battery charging and discharging current will be due to the power provided by the photovoltaic panel. A triangular signal is given as solar irradiation which will change the power produced by the photovoltaic panel.

From T = 0 - 1.3 s the battery will charge by the buck operation of the bi-directional converter, as the power provided by the PV array is more than the power required by the load. Now at T=1.3 s the battery will start discharging by the boost operation of the bi-directional converter, and the power supplied by the battery will gradually increase till T = 2 s as the irradiance is decreasing till T = 2 s. After T = 2 s the irradiance will increase and at T = 2.5 s the power supplied by PV array will become more than required by the load and hence the battery will start charging and charge till T = 6 s as shown in Figure 5.4. After that the battery will again discharge as the power required by the load is more than that supplied by the PV array.

During all these operations the voltage of the DC bus is maintained constant at 24 V refer Figure 5.6. Since the photovoltaic panel is controlled by MPPT algorithm the power characteristics of the PV panel will be similar to the solar irradiation characteristics. The change in battery charging and discharging current can be seen in Figure 5.5.

5.3.2 Variable Load

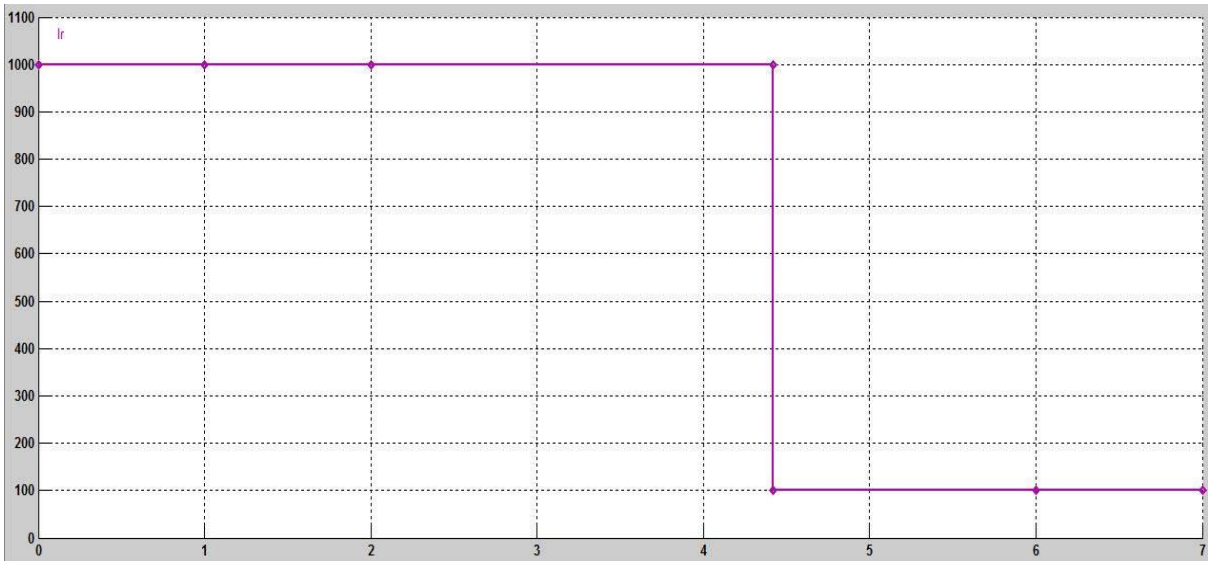

Figure 5.7 Constant Irradiance (100W/m2 – 1000W/m2).

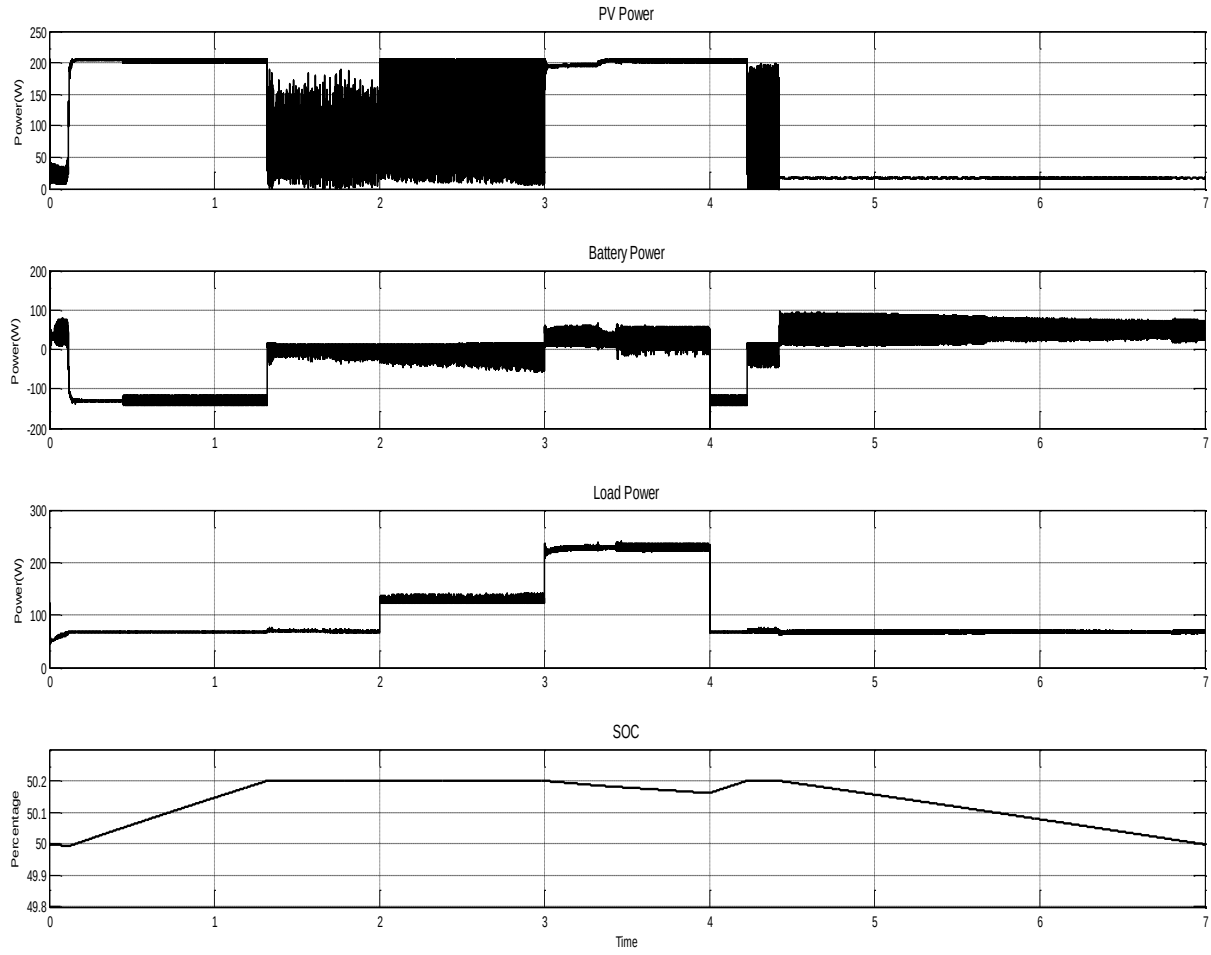

Figure 5.8 Power and SOC waveforms corresponding to variable Load.

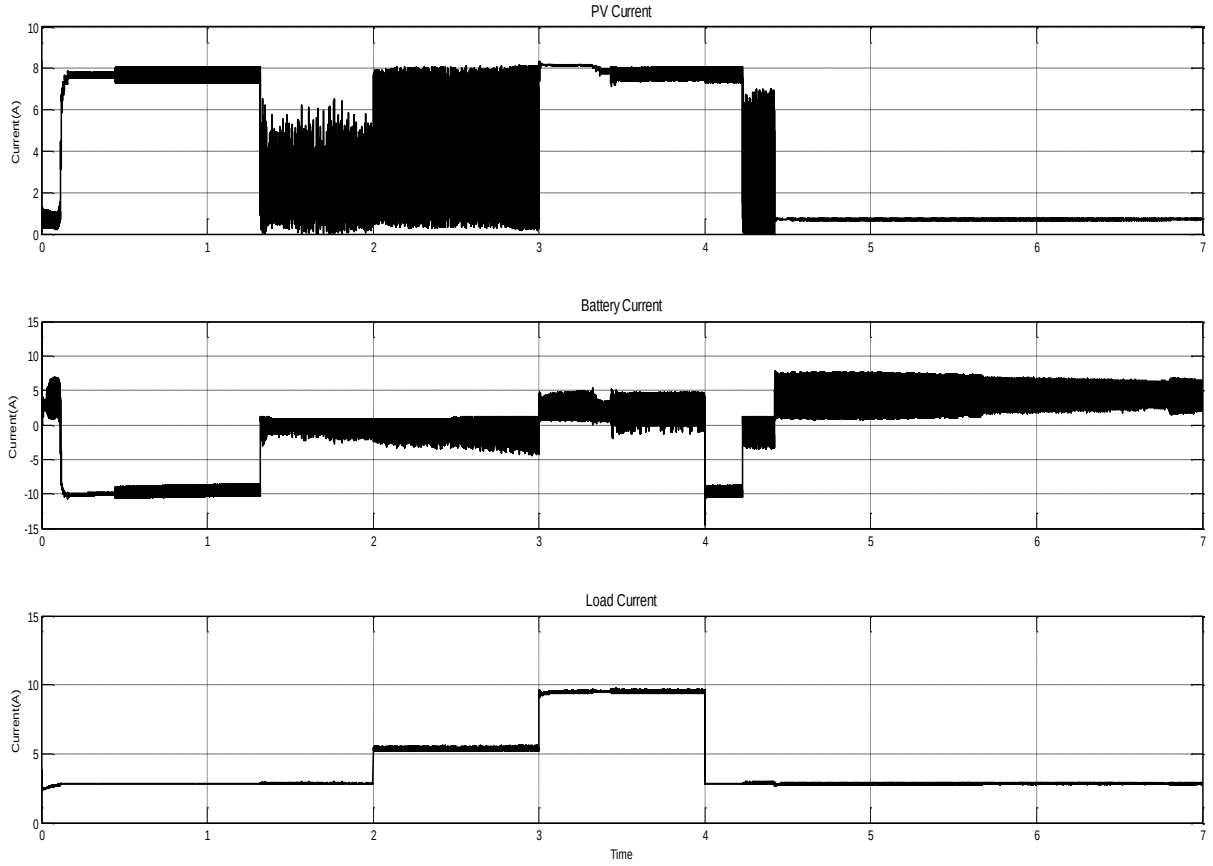

Figure 5.9 Current waveforms corresponding to variable load.

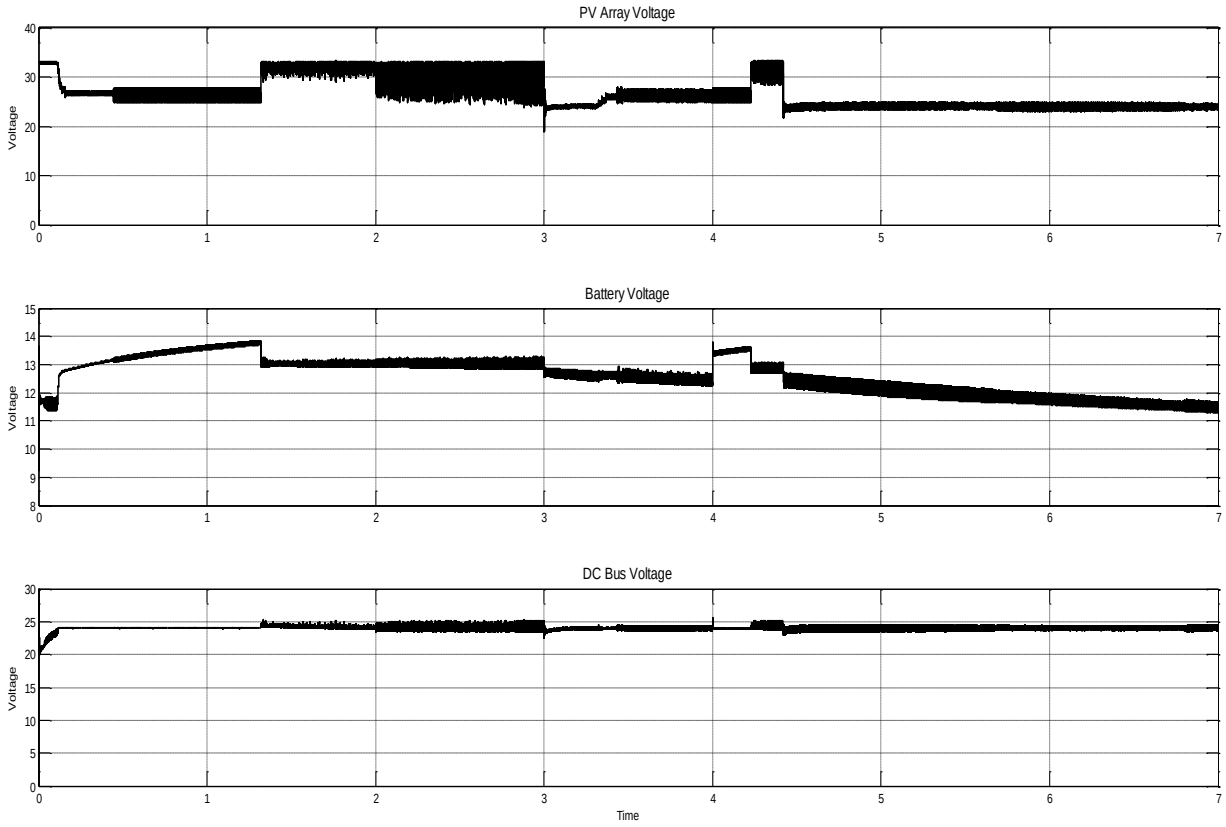

Figure 5.10 Voltage waveforms corresponding to variable Load.

A resistive load is connected which is varied in three steps. A constant solar irradiation is provided to the PV panel which is changed in step from 1000W/m^2 to 100 W/m^2 at T= 4.4 s as shown in Figure 5.7.

From T = 0 s to T = 2 s the load is 8.5 Ω and since the power supplied by the PV array during this period is more than that required by the load. So the battery will start charging by the buck operation of the bi-directional converter and at T = 1.3 s the battery reaches the full charge condition. At this point the duty cycle of the switch responsible for buck operation is made 0 and the control of buck converter connected directly to the PV array, is passed from MPPT controller to PI controller as we no longer require the maximum power as shown in Figure 5.8.

Now by the time PI controller adjusts the power supplied by the PV array to match the load, the battery will discharge slightly to maintain the constant DC bus voltage thus fulfilling the deficit between the load and source power. Due to this slight discharge the control is again shifted to the MPPT controller and battery is again charged to its full value. This results in the fluctuation of current supplied by the PV array but all this does not affect the load side as the load gets the desired power and DC bus voltage is maintained constant.

At T = 2 s the load is reduced to 4.5 Ω so the power demanded by the load increases. But the power requirement by the load is still less than the maximum power PV array can supply and hence the behavior of the PV current from T = 2 s to T = 3 s will be same as that in the interval T = 1.3 s to T = 2 s. At T = 3 s the load is further reduced to 2.5 Ω and hence the power demanded by the load becomes more than the PV array could supply. Therefore for interval T = 3 s to T = 4 s the battery will discharge and supply power to the load.

At T = 4 s the load is again increased to 8.5 Ω and hence the power demanded by the load becomes less than the PV array power therefore the battery will start to charge. At T = 4.2 s the battery again gets fully charged and will remain charged until T= 4.4 s when the irradiance is reduced to 100 W/m^2 the power supplied by the PV array becomes less than required by the load and hence the battery discharges from T = 4.4 s to T = 7 s. Change is load current is observed at all the three steps as shown in Figure 5.9. During all these operation the DC bus voltage is maintained at 24 V as shown in Figure 5.10.

5.3.3 Speed Control of DC Motor

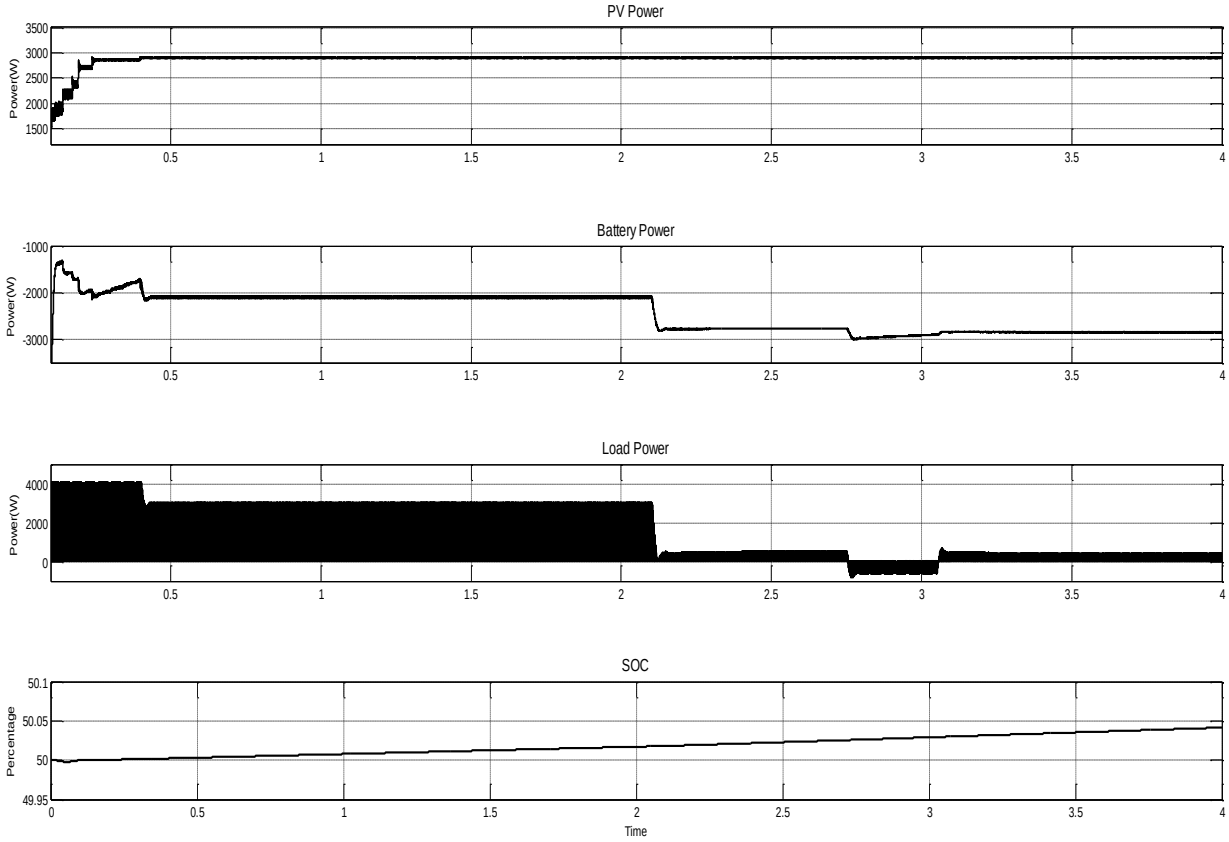

Figure 5.11 Power and SOC waveforms with DC motor as load.

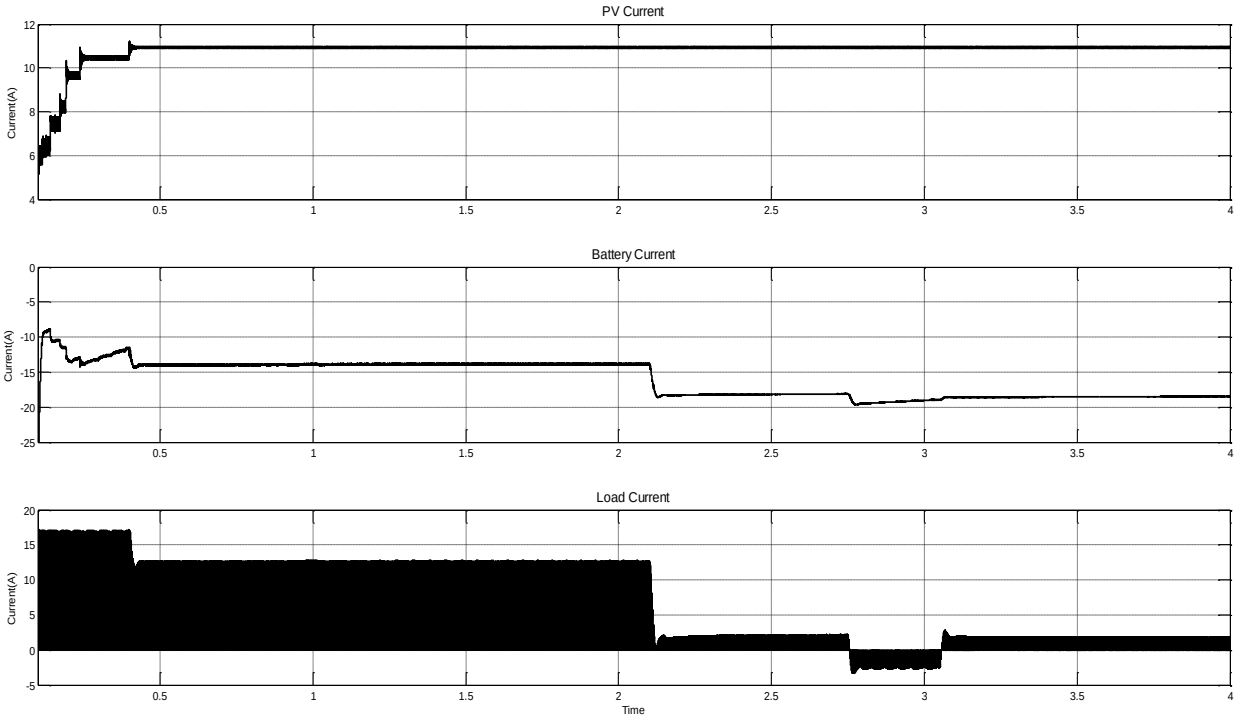

Figure 5.12 Current waveforms with DC motor as load.

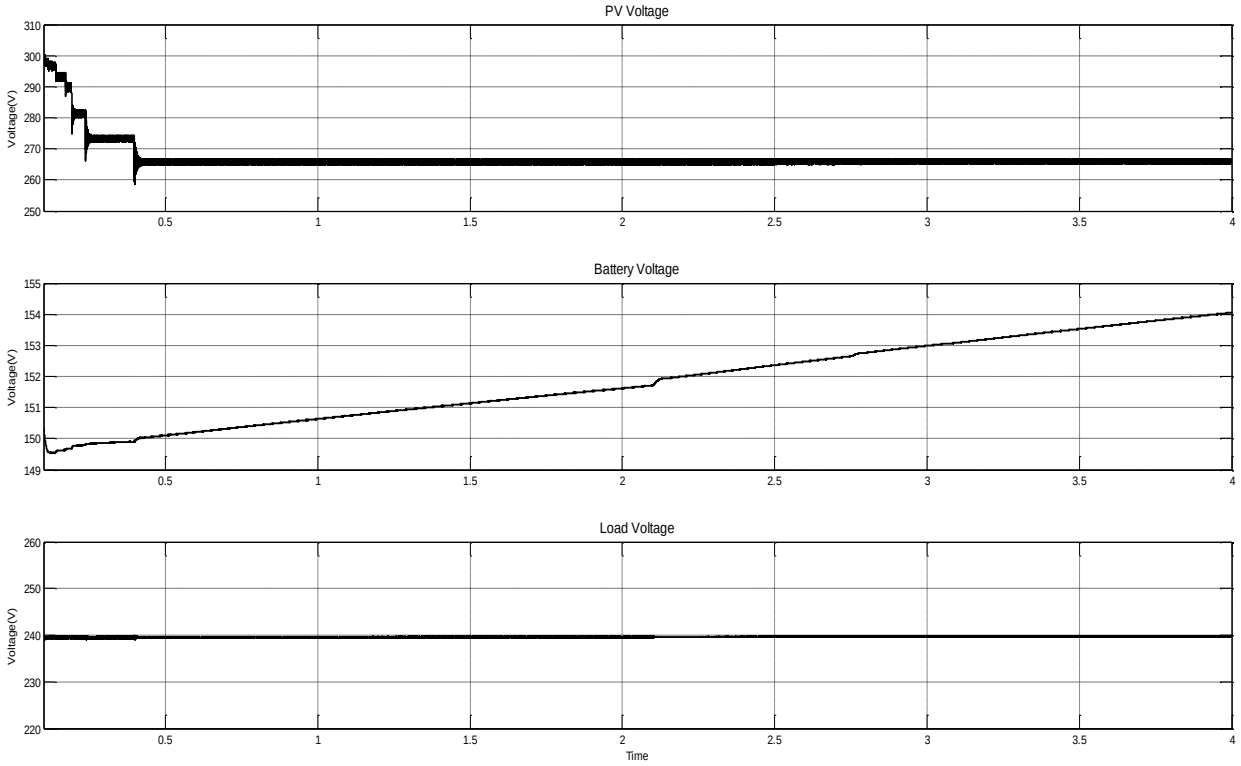

Figure 5.13 Voltage waveforms with DC motor as load.

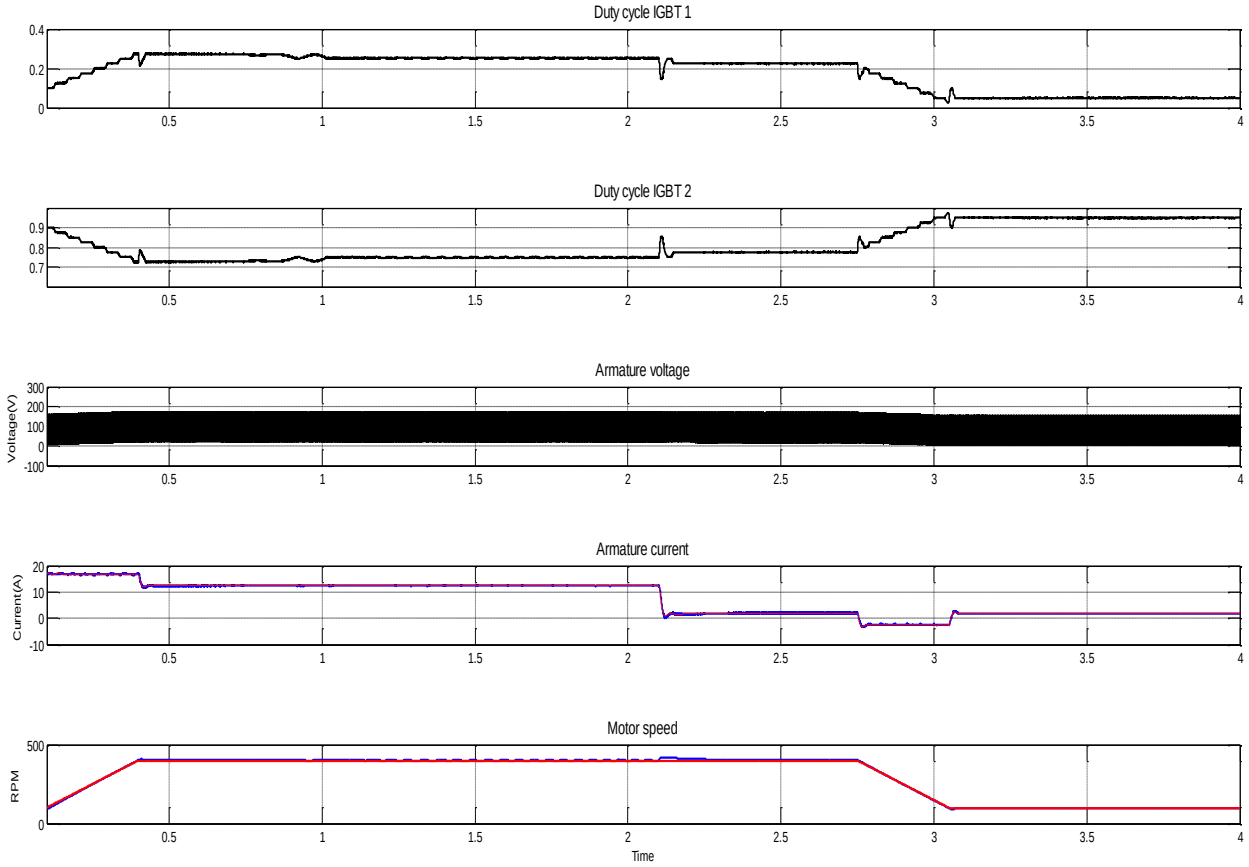

Figure 5.14 Motor performance waveforms with DC motor as load.

5 HP 240 V separately excited DC motor is connected at port 3 as load via a two-quadrant chopper which operates such that the motor acts as load and source both. The photovoltaic panel is provided a constant irradiance of 500 W/m^2. The panel used in this simulation has V_{mp} = 265V and I_{mp} = 11 A at the given environmental conditions. Thus the photovoltaic panel produces 3kW power as shown in Figure 5.11. The battery has a nominal voltage of 150 V and capacity of 40 Ah.

The DC motor starts from rest. Reference speed is set at 400 rpm but to prevent the over reference current a 1000 rpm/s acceleration ramp is provided. Initially a load torque of 15 Nm is also applied. Under the given condition the machine starts to accelerate and reaches the steady state at T = 0.4 s. Since during this region (T = 0 to 0.4 s)the power required by the motor is less than that supplied by the photovoltaic panel the bidirectional converter will operate in buck mode and charge the battery refer Figure 5.11 and Figure 5.14.

Since the motor stop accelerating at T = 0.4 s, a drop in load current is observed as shown in Figure 5.12. This current is added to the battery charging current to maintain the constant DC bus voltage of 240 V. From T = 0.4 s to T = 2.1 s the motor will be in steady state at 400 rpm. At T = 2.1 s the load torque is dropped to 2 Nm thus reference current of the motor will drop to maintain a constant speed of 400 rpm. Again due to the drop in load current, the battery charging current will increase.

At T = 2.75 s the reference speed is dropped to 100 rpm. The motor is deaccelerated via a ramp of 1000 rpm/s to prevent large regenerative currents. Since the motor is deaccelerating the kinetic energy of the motor is converted to the electrical energy by regenerative braking and the energy recovered is fed back to the battery via buck mode of the bidirectional converter.

At T = 3.15 s the motor speed will be 100 rpm, in order to maintain the constant speed and overcome the load torque motor will require power and the load current will again become positive. This positive current will be deducted from the battery charging current since a constant power is supplied by the photovoltaic panel.

During whole process the DC bus voltage is maintained constant at 240 V as shown in Figure 5.13. The photovoltaic will operate at maximum power point to achieve maximum output. Motor actual speed and current will follow the reference speed and current respectively as shown in Figure 5.14.

CHAPTER 6: HARDWARE DEVELOPMENT

In this chapter, three-port converter circuit was modelled to verify the operation of the circuit under different input conditions. In this chapter, the development of hardware prototype of the circuit is presented. A description of every component used to realize the power and control part of the circuit is covered here along with the results and inferences.

6.1 Hardware Setup

A three-port bidirectional DC-DC converter circuit was realized using switches, sensing circuits and a controller. The developed circuit had a provision to interface a source, battery and load. A variable DC supply was used as the source. Lead acid batteries were used, since they are easier to handle, cheaply available and not too sensitive to operating conditions. A rheostat with current rating of 5A is used as the load.

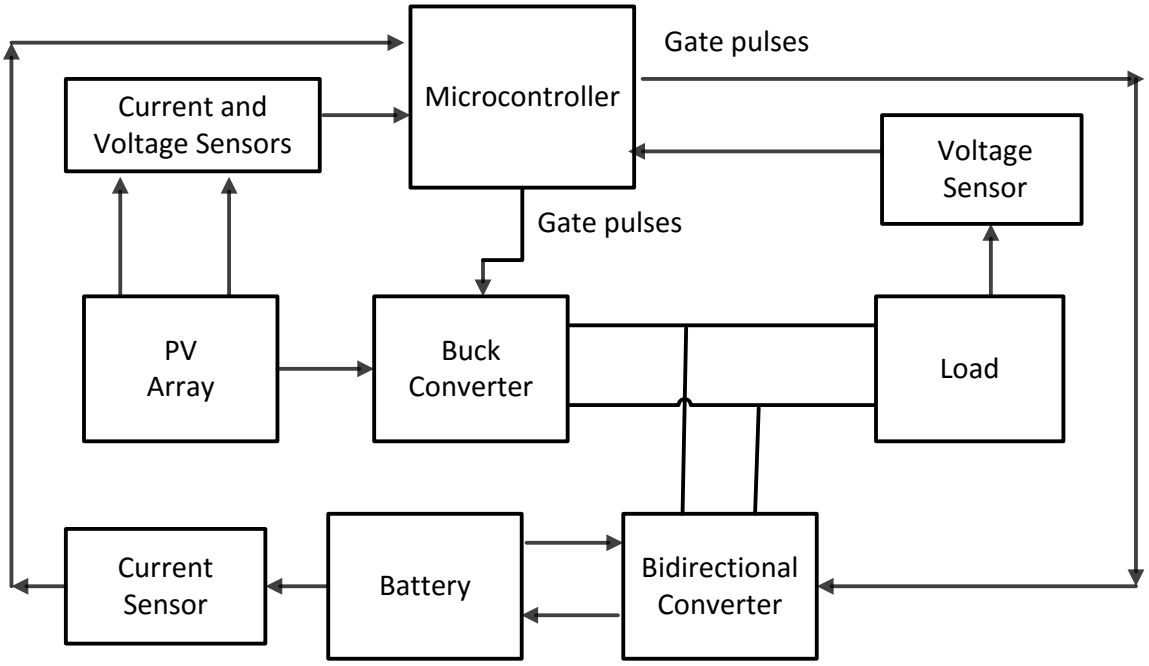

Figure 6.1 Block diagram of hardware setup.

The unidirectional paths between the source and the DC bus was realized by Buck converter, comprising of power MOSFET, power diode and inductor. The bidirectional path between the battery and DC bus is realized using two MOSFETs and an inductor. To determine

the state of charge and current of battery, current sensing circuits were used in series with the battery. A voltage and current sensor is used to measure the PV parameters so that it can operate at MPPT. A voltage sensor is used to measure the DC bus voltage to implement the control of bidirectional converter. Lastly, the control algorithm and gate signals for switches were generated using a microcontroller. Each of the components of the setup is described in the following sections along with their specifications.

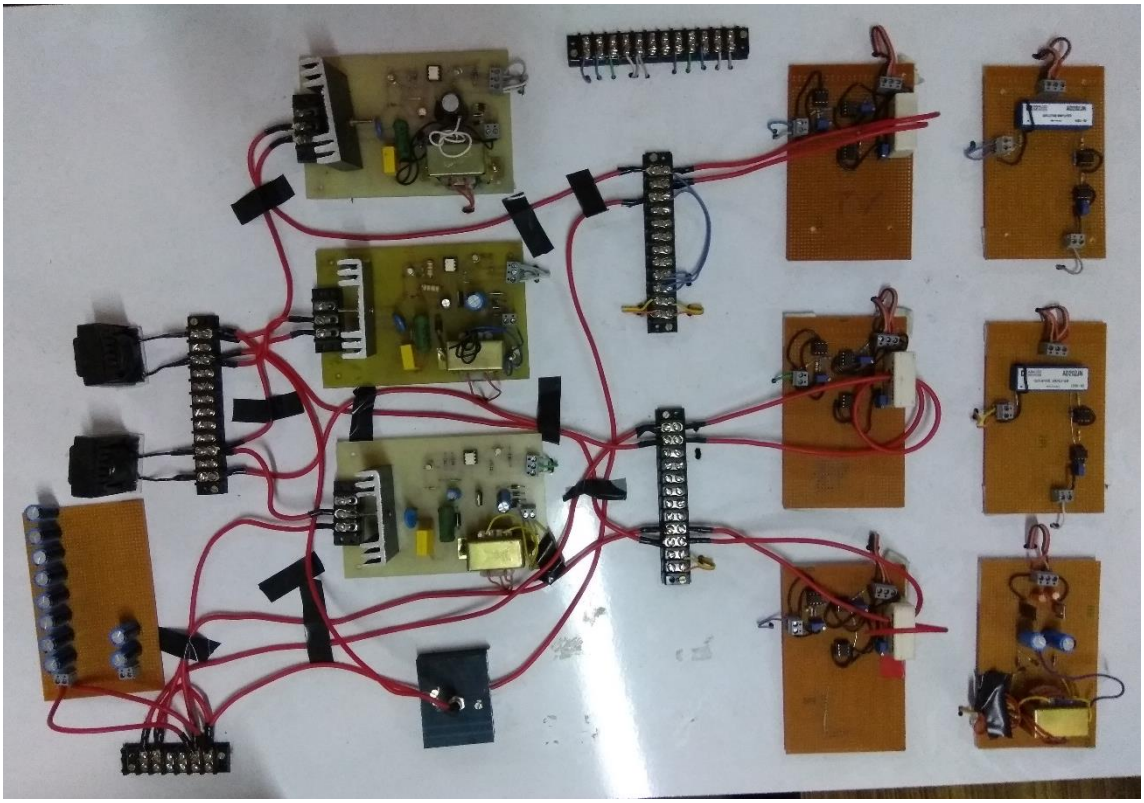

Figure 6.2 Complete hardware setup (offline).

6.1.1 Batteries

Lead acid batteries were used in the circuit to store the energy supplied by the source. Commonly lead acid batteries are only used for such applications as lead acid batteries are cheap, safe and easy to handle as well as robust enough to handle small amount of mal operation. The specifications of the batteries are as follows:

- Nominal Voltage = 12V
- Capacity 7.2 Ah at 20 Hr

Figure 6.3 Lead acid battery used in the circuit.

6.1.2 Switches

Three switches were developed for the three-port converter circuit. The switches were used to make buck converter and bidirectional converter. The MOSFET used in this circuit is IRFP460. The specifications of the MOSFET are as follows:

- Maximum drain source current: 20A
- Maximum drain source voltage : 500V
- Drain source resistance : 0.27 ohm

A power diode rated 16A is used in the buck converter. The pulse amplification and isolations circuit forms the MOSFET gate driver circuit.

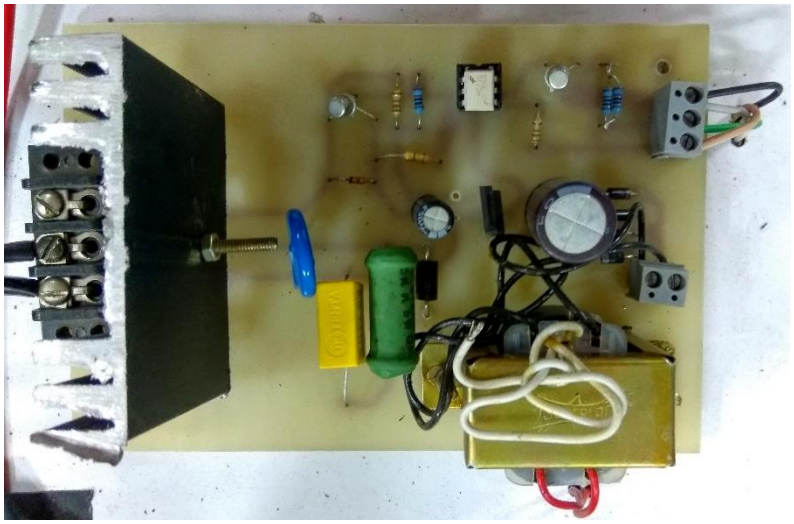

Figure 6.4 Driver circuit of switch.

6.1.3 Pulse Amplification and Isolation Circuit

Power MOSFETs used in the circuit require a gate source switching signal of 12V. However the control circuit generally generates a low voltage signal (5V in this particular case). Thus, pulse amplification and isolation circuits are required. The optocoupler MCT2E is used to isolate the high voltage power circuit from the low voltage control circuit. As shown in the figure, the input transistor conducts when current flows through the base from the 5V switching signal. When this signal is high, the input transistor goes into saturation and LED of the optocoupler glows. The photo transistor in the MCT2E thus saturates and connects the base directly to the emitter of the output transistor. The output transistor goes into cut- off and this allows the gate terminal to pull up to 12 V. The input and output transistors used in this circuit are 2N2222.

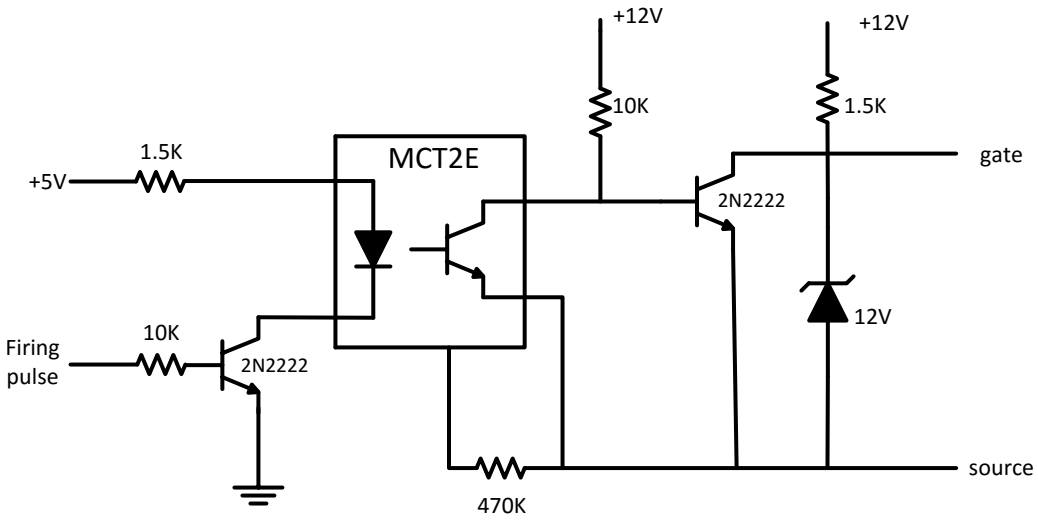

Figure 6.5 Pulse Amplification and Isolation Circuit.

6.1.4 Snubber Circuit

When switching MOSFETs at high frequencies, the current and voltage transients can exceed the rated value. To protect the MOSFET from high (di/dt) and (dv/dt), snubber circuits are used. Snubber circuit consists of a high power snubber resistance and capacitor In addition to this, a Metal Oxide Varister (MOV) is used to protect the switch from over voltage.

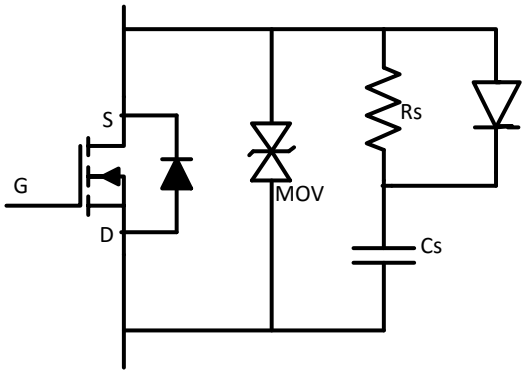

Figure 6.6 Snubber circuit for MOSFET protection.

6.1.5 Current Sensing Circuit

To obtain feedback in the circuit, current sensors have been used to estimate the State of Charge of the batteries. In addition to this, the current sensors have also been used to measure currents flowing through the switches and the inductor. The current sensor used is HTP25 with arrange to measure 25A current in either direction. This is basically a Hall Effect sensor that also provides galvanic isolation between its output (control circuit interface) and input (power circuit). If N_p turns of the input current carrying wire I are wound on the sensor, then the sensor transforms this current at the output as ($N_pI/1000$). Using a resistance R_o across the output terminals, the current is converted to a suitable voltage. In order to interface this voltage with the microcontroller input pin, 3 levels of op-amp gain circuits are connected to the output of the sensor.

- A buffer circuit is used to improve the drive of the output signal.
- A scalar is used to provide a suitable constant gain. The gain is adjusted by selecting the proper feedback resistance
- An adder circuit to add a fixed offset to the output. This is required when it is desired to measure bi-directional current bipolar output but the microcontroller ADC can only take unipolar input.

The current sensors were tuned using potentiometers. The adder is used to provide an offset of 2.5 volts. The scalar is used to set the gain so that greater magnitude among I_{max} and I_{min} corresponds to 5V or 0V respectively.

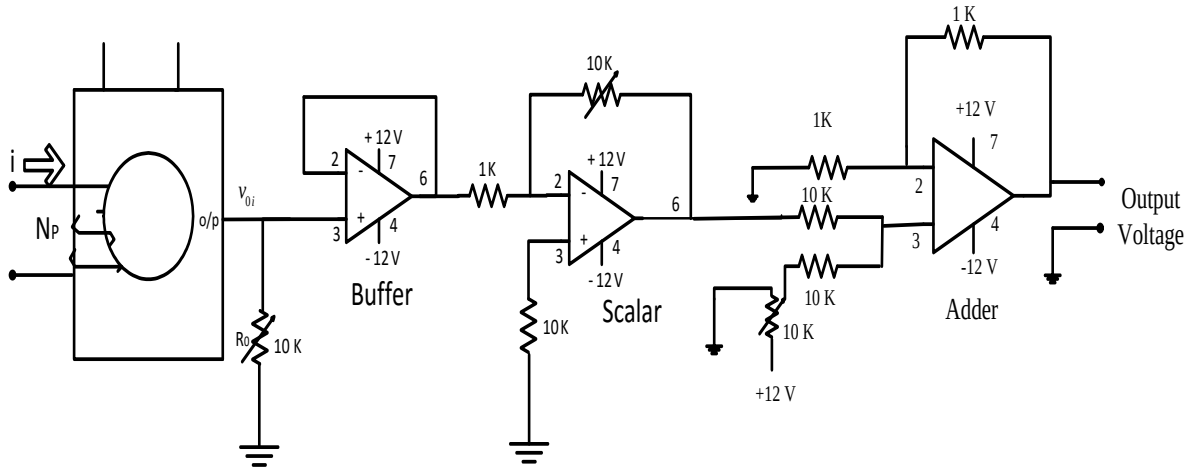

Figure 6.7 DC current sensor circuit.

6.1.6 Voltage Sensing Circuit

It is an important circuit needed for close loop operation of control scheme. Sensor output is processed using a unity gain buffer and an inverting amplifier. Input Resistors are used to scale down the voltage within the range of AD202 (isolation amplifier). Op-amp circuits are used at the output of AD202 for adjusting the scale. Circuit diagram of Voltage sensing circuit is shown in Figure 6.8.

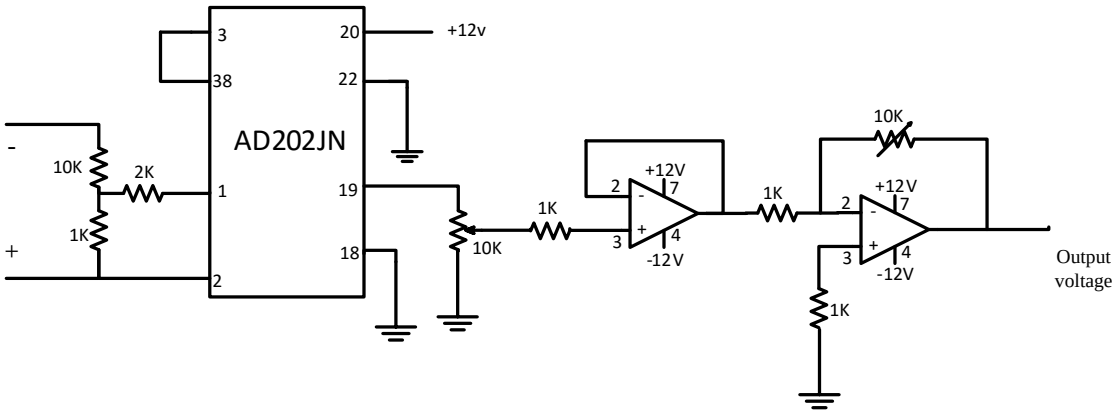

Figure 6.8 DC voltage sensing circuit.

6.1.7 Power Supply

Dc Regulated supplies (+12V, gnd, -12V and +5V) are required for providing biasing to various circuits like pulse amplification and isolation circuits, voltage sensing circuits, current sensing

circuits etc. using ICs 7812 for +12V, IC 7912 for -12V, and 7805 for +5V. The circuit diagram of the regulated DC power supplies are shown in Figure 6.10.

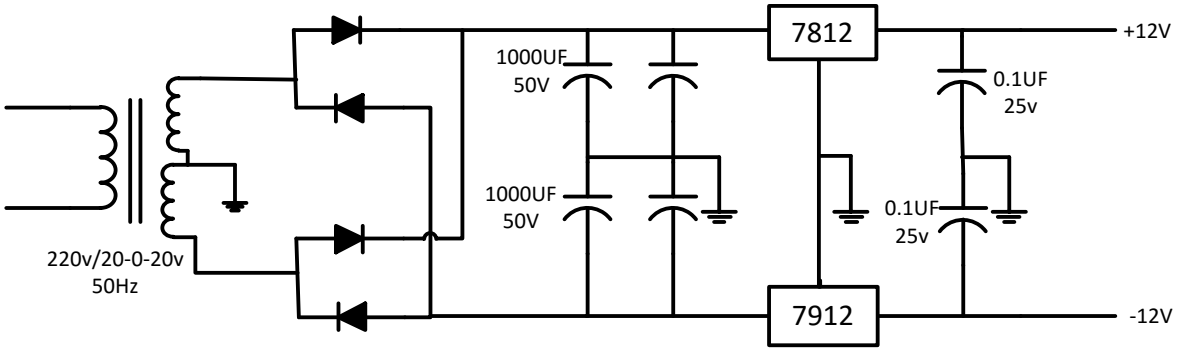

Figure 6.9 Circuit diagram of +12V, -12V supply.

6.1.8 Microcontroller

To generate gate signals for switches and to control the state machine of the circuit operation i.e. changing between equalizing and dead phase, a digital microcontroller was used. The Arduino Mega 2560 is a microcontroller board based on the ATmega 2560. The on chip peripherals on the board include54 digital I/O pins, 16 analog inputs interfaced with the ADC on board. The relevant technical specifications are as follows:

- It is a 5V digital system.
- It consists of a 10 bit ADC and hence provides an input analog voltage resolution of 5/1024 = 0.049 V, which is sufficient to measure all dynamic changes in the balancer circuit.
- It has a 16MHz clock which is more than sufficient to generate switching gate pulses on the digital pins of about 10kHz

The programs written in the controller to perform various tasks are presented in the appendix.

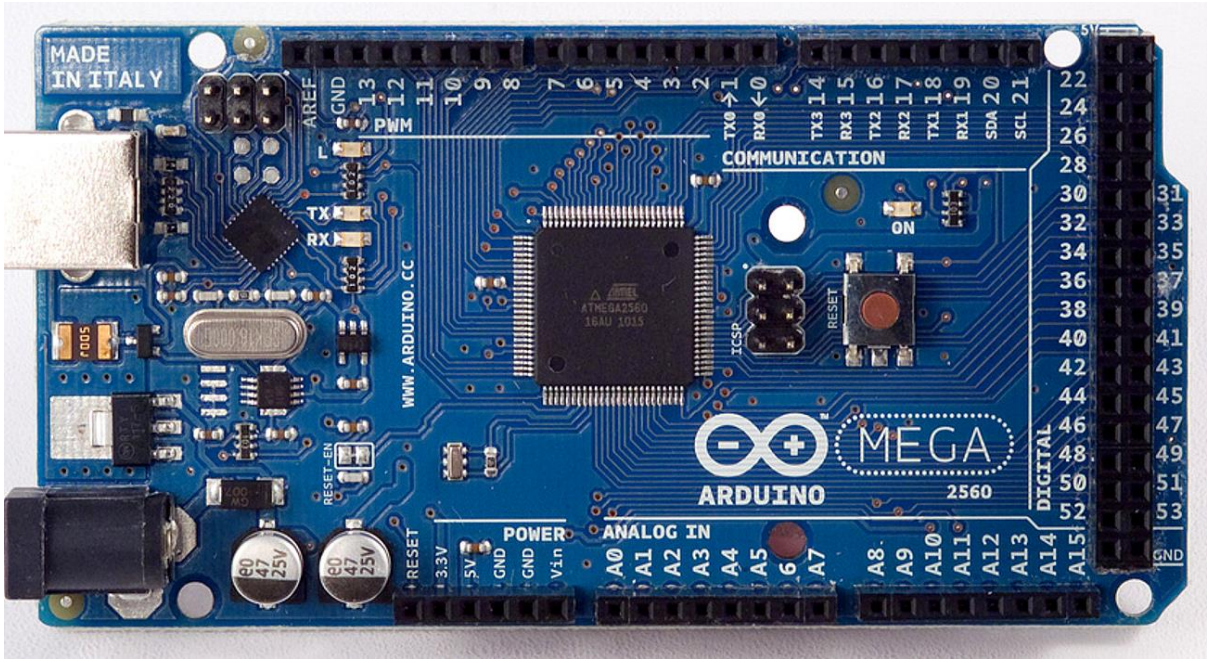

Figure 6.10 Arduino mega 2560 microcontroller.

6.2 Hardware Results

The buck and boost converter of the bidirectional converter is tested. 12V lead acid battery is used as the source and rheostat as load. The operating frequency of the converter was 3 kHz and the duty cycle was set at 0.4. An inductor of 5mH and capacitor of 8uF was used to maintain the continuous mode of the converter.

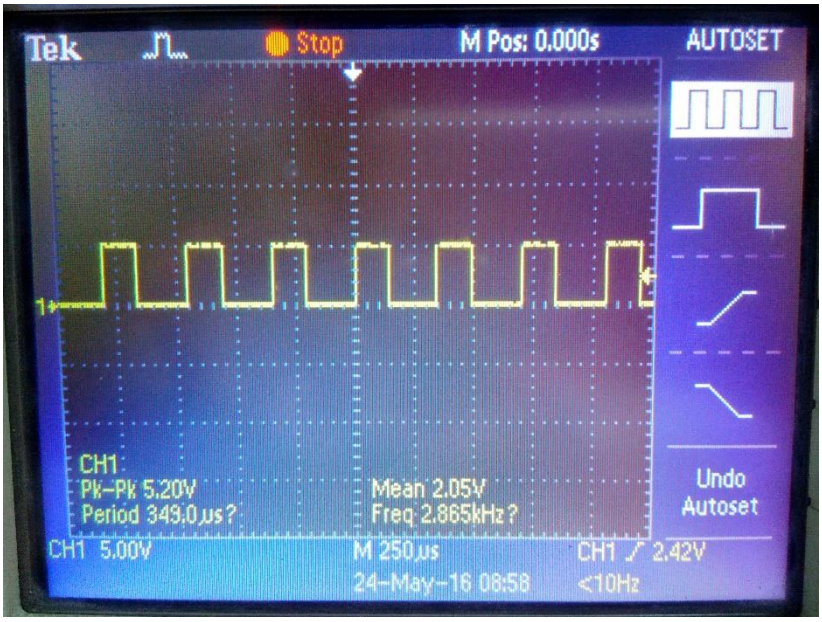

Figure 6.11 Applied duty cycle waveform.

6.2.1 Buck Converter

Buck converter operating in continuous mode provides following output voltage:

$$V_o = D.V_{in} \tag{6.1}$$

V_{in} = 12.4 V, voltage of the lead acid battery,

D = 0.4.

Therefore V_o = 4.96 V, in Figure 6.12 the blue waveform represents the input voltage and the output voltage is represented by the yellow waveform. As the practically obtained values are equal to the theoretically calculated values, the buck converter is working properly.

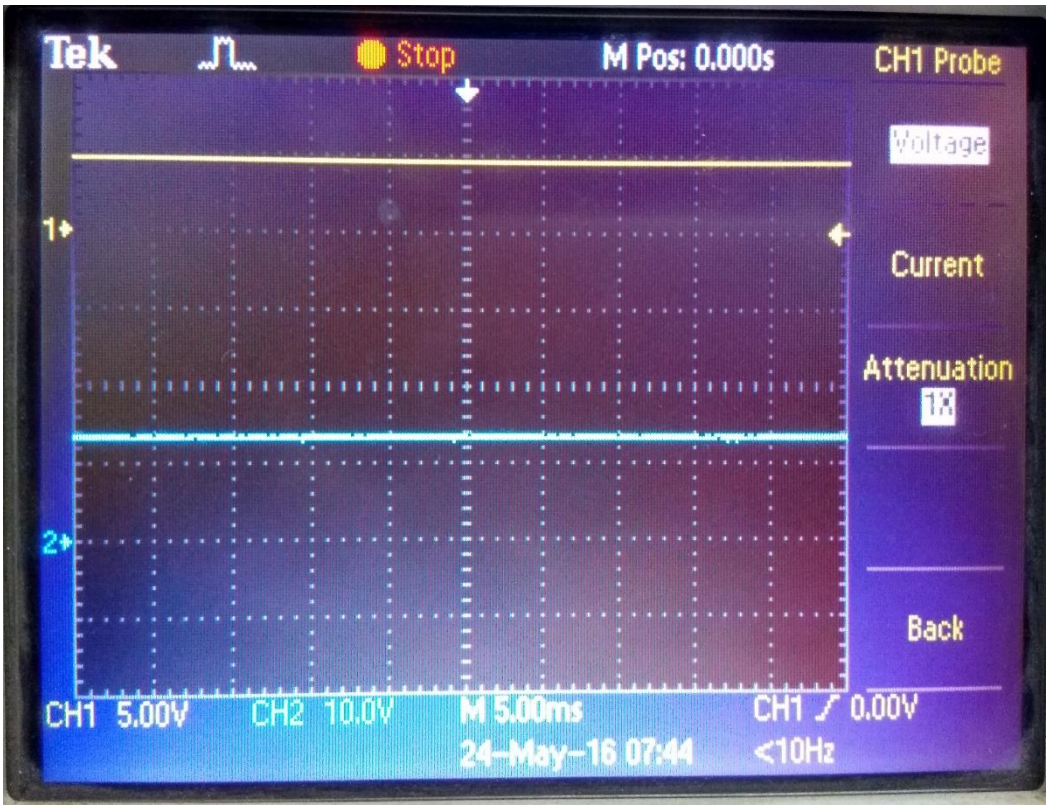

Figure 6.12 Results of buck converter.

6.2.2 Boost Converter

Boost converter operating in continuous mode provides following output voltage:

$$V_o = \frac{V_{in}}{1-D} \tag{6.2}$$

V_{in} = 12.4 V, voltage of the lead acid battery,

D = 0.4.

Therefore V_o = 20.66 V, in Figure 6.13 the blue waveform represents the output voltage and the input voltage is represented by the yellow waveform. As the practically obtained values are equal to the theoretically calculated values, the boost converter is working properly.

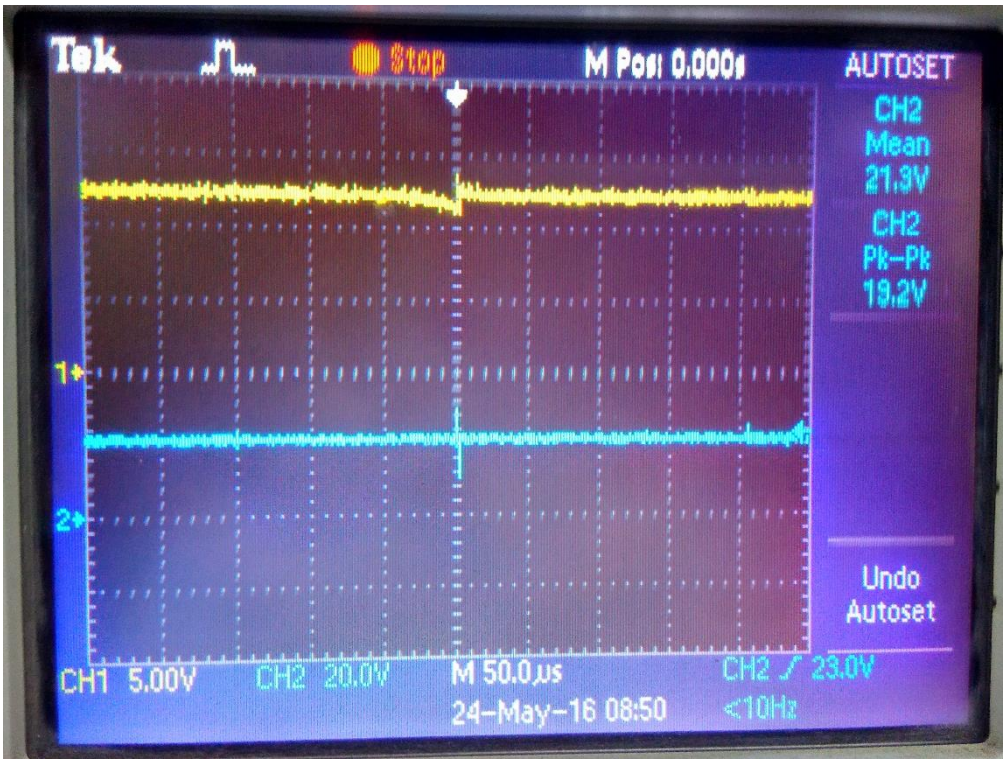

Figure 6.13 Results of boost converter.

CHAPTER 7: CONCLUSION AND FUTURE SCOPE

This report provides the potential application of Multi-port converters in Hybrid Electric vehicles. They are required to manage the power flow between all the on-board renewable sources, storage units and load. Mathematical model of the photovoltaic panel has been discussed and the varying P-V and I-V characteristics under changing environmental conditions has been studied. Different MPPT techniques are analyzed and is used to harness the maximum power from the photovoltaic panel.

The limitations of the traditional two-port converters are described and a three-port bidirectional DC-DC converter topology is proposed in the report. Three-port bidirectional converter topology interface a photovoltaic cell, battery and DC load. Control strategy of the buck converter using MPPT algorithm and PI control of the bi-directional converter to charge and discharge the battery according to the power supplied by the photovoltaic is also discussed.

Simulations of the proposed porotype is carried out under resistive load and separately excited DC motor. Results for variable irradiance and variable load shows desired operation of the multi-port converter. DC bus voltage is maintained constant and PV array power characteristics follow the irradiance curve thus proving the maximum power flow from Photovoltaic array. The simulation results verify that the prototype can be scaled according to the application and can be employed in hybrid electric vehicles. Multi-port converters increase the overall efficiency of the system by implementing the regenerative braking in hybrid electric vehicle.

More renewable sources of energy can be incorporated to provide an uninterrupted power from the renewable sources, for example full cells can be connected for hybrid vehicles application in a four-port converter topology. Other converter topologies providing galvanic isolation can be used for better performance under conditions when the difference in voltage levels between sources and loads is large.

PUBLICATION

[1] Sarvagya Agrawal and Dr. S. P. Singh “Multi-port converter for Solar powered Hybrid vehicle”, 43rd IEEE Photovoltaic Specialists Conference (2016), Accepted.

REFERENCES

[1] V. M.Pacheco, L. C.Freitas, J. B.Vieira, E. A.Coelho, and V. J.Farias, "Stand-alone photovoltaic energy storage system with maximum power point tracking," Proc. IEEE APEC, 2003, pp. 97 -102.

[2] S. Janjornmanit, S.Panta, "Novel battery charging and discharging control system for solar panel using one-by-one controllers and maximum power point tracker", IEEE, 2005, pp 2.

[3] H. Tao, J.L. Duarte, M.A.M. Hendrix, "Multiport converters for hybrid power sources", Proc. IEEE Electromechanics and power electronics, 2008, pp 3413-3416.

[4] A. Di Napoli, F. Crescimbini, L. Solero, F. Caricchi, F.G. Capponi, "Multiple-Input DC-DC power converter for power-flow management in hybrid vehicles", IEEE, 2002, pp 1578-1580.

[5] V.V. Vincent, S. Kamalakkannan, "Advanced hybrid system for solar car", IEEE ICCPEIC, 2013, pp 23-24.

[6] W. Hu, H. Wu, Y. Xing, K.Sun, "A full-bridge three-port converter for renewable energy application", IEEE Transaction on power electronics, 2014, pp 57-59.

[7] S.W. Mohod, S.D. Deshmukh, "DC-DC converter for interfacing energy storage", AIJRSTEM, 2013, pp 79-81.

[8] B. Dhivya, S. Dhamodharan, "Analysis of multiport DC-DC converter in renewable energy sources", IJRET, 2013, pp 181-182.

[9] Chen Cha, H. Lee, "Design and Implementation of Photovoltaic Power Conditioning System using a Current based Maximum Power Point Tracking," Proc. of 43rd IEEE IAS, 2008, pp. 1-5.

[10] Mohammad A.S. Masoum, Hooman Dehbonei, "Theoretical and Experimental Analyses of Photovoltaic Systems With Voltage-and Current-Based Maximum Power-Point Tracking," IEEE Transactons of Energy Conversin, Vol. 17, No.4, December 2002.

[11] S.Duryea, S.Islam, and W. Lawrance, "A battery management system for stand-alone photovoltaic energy systems," IEEE Industry Applications Magazine, 2001, 7(3), pp.67-72.

[12] E. Koutroulis and K. Kalaitzakis “Novel battery charging regulation system for photovoltaic applications,” IEE Proc. Electr. Power Appl., vol 151, no. 2, pp. 191-197, Mar. 2004.

[13] H. Matsuo and F. Kurokawa, “New solar cell power supply system using a boost type bidirectional dc-dc converter,” IEEE Trans. Ind. Electron., vol. IE-31, no. 1, pp. 51-55, Feb. 1984.

[14] R. J. Wai and R. Y. Duan, “High-efficiency bidirectional converter for power sources with great voltage diversity,” IEEE Trans. Power Electron., vol. 22, no. 5, pp. 1986-1996, Sep. 2007.

[15] B. G. Dobbs and P. L. Chapman, “A multiple-input DC-DC converter topology,” in Proc. IEEE Power Electron. Lett., Mar, 2003, vol. 1, pp. 6– 9.

[16] Z. Qian, O. Abdel-Rahman, H. Al-trash, and I. Batarseh, “Modeling and control of three-port DC/DC converter interface for satellite applications, IEEE Trans. Power Electron., vol. 25, no. 3, pp. 637–649, Mar. 2010.

[17] Bhatnagar, Pallavee, and R. K. Nema. "Maximum power point tracking control techniques: State-of-the-art in photovoltaic applications." Renewable and Sustainable Energy Reviews 23 (2013): 224-241. APA.

[18] Tao, H., Kotsopoulos, A., Duarte, J. L., & Hendrix, M. A. (2006, May). Family of multiport bidirectional DC-DC converters. In Electric Power Applications, IEE Proceedings- (Vol. 153, No. 3, pp. 451-458). IET.

[19] Mihai, Mihaescu. "Multiport converters-a brief review." Electronics, Computers and Artificial Intelligence (ECAI), 2015 7th International Conference on. IEEE, 2015.

[20] Zhao, Chuanhong, Simon D. Round, and Johann W. Kolar. "An isolated three-port bidirectional DC-DC converter with decoupled power flow management." Power Electronics, IEEE Transactions on 23.5 (2008): 2443-2453.

[21] Kolluru, Venkata Ratnam, Kamalakanta Mahapatra, and Bidyadhar Subudhi. "A new approach to fast tracking and low cost single exponential model photovoltaic system." Microelectronics and Electronics (PrimeAsia), 2013 IEEE Asia Pacific Conference on Postgraduate Research in. IEEE, 2013.

[22] Pires, V. Fernão, et al. "Power converter interfaces for electrochemical energy storage systems–A review." Energy Conversion and Management 86 (2014): 453-475.

[23] Velasco De La Fuente, David, et al. "Photovoltaic power system with battery backup with grid-connection and islanded operation capabilities." Industrial Electronics, IEEE Transactions on 60.4 (2013): 1571-1581.

[24] Rahmani, S., et al. "A multifunctional power flow controller for photovoltaic generation systems with compliance to power quality standards." IECON 2012-38th Annual Conference on IEEE Industrial Electronics Society. IEEE, 2012.

[25] Qian, Zhijun, et al. "Small signal modeling of a compound Half-bridge DC/DC converter for renewable energy applications." Telecommunications Energy Conference (INTELEC), 32nd International. IEEE, 2010.

[26] Caricchi, F., et al. "Experimental study of a bidirectional DC-DC converter for the DC link voltage control and the regenerative braking in PM motor drives devoted to electrical vehicles." Applied Power Electronics Conference and Exposition, 1994. APEC'94. Conference Proceedings 1994, Ninth Annual. IEEE, 1994.

[27] Murty, Balarama V., and Chandra S. Namuduri. "Single current regulator for controlled motoring and braking of a DC-fed electric motor." U.S. Patent No. 5,291,106. 1 Mar. 1994.

APPENDIX

A. Parameters of DC Motor

Type	Separately excited
Rated Power	5 HP
Rated Speed	1750 rpm
Mutual Inductance	1.234 H
Armature Voltage	240 V
Armature Resistance	0.78 Ω
Armature Inductance	0.016 H
Field Voltage	150 V
Field Resistance	150 Ω
Field Inductance	112.5 H
Moment of Inertia	0.05 kg-m^2
Viscous friction coefficient	0.01 N-m-s

Table 1. Separately excited DC machine parameters.

B. Control Parameters

Buck K_p	7
Buck K_i	1
Bidirectional Buck K_p	40
Bidirectional Buck K_i	4
Bidirectional Boost K_p	0.1
Bidirectional Boost K_p	2
Motor speed controller K_p	60
Motor speed controller K_i	400
Motor current controller K_p	2
Motor current controller K_i	200

Table 2. Control parameters of the circuit.

C. PV array characteristics

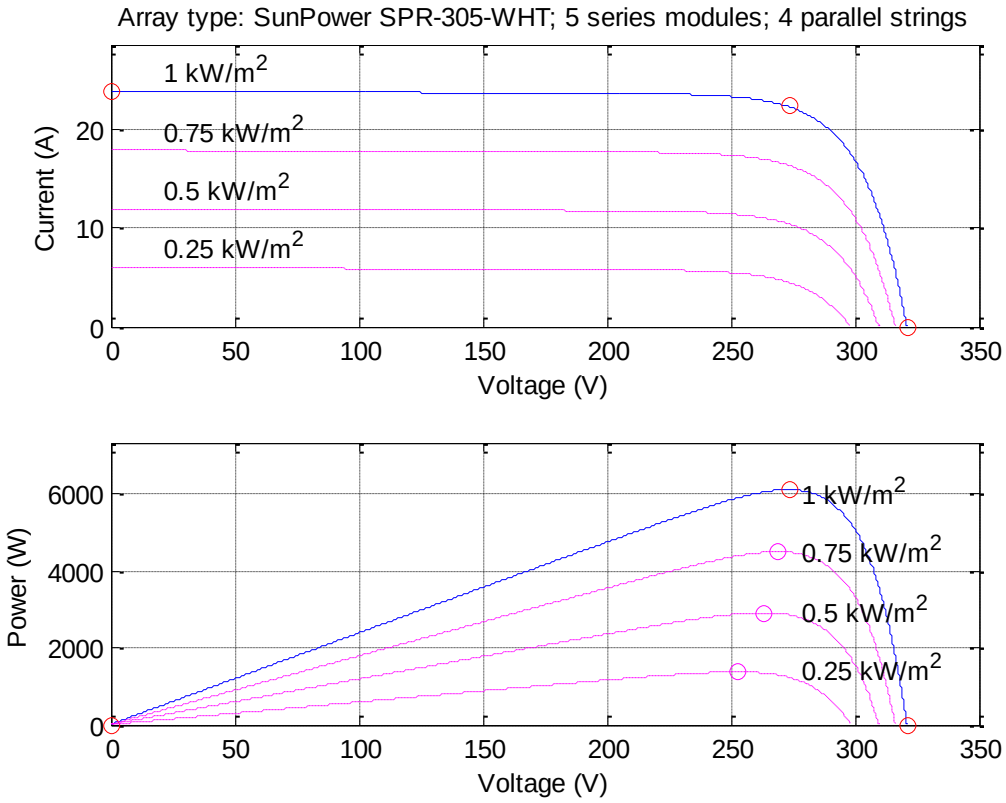

Figure c. P-V and I-V characteristics of photovoltaic array.